Coordination Chemistry Reviews 293–294 (2015) 228–249

Contents lists available at ScienceDirect

Coordination Chemistry Reviews

journal homepage: www.elsevier.com/locate/ccr

Review

Electroluminescence from europium(III) complexes

Hui Xu[a,*], Qiang Sun[b], Zhongfu An[b], Ying Wei[a], Xiaogang Liu[b,c,**]

[a] Key Laboratory of Functional Inorganic Material Chemistry, Ministry of Education and School of Chemistry and Materials, Heilongjiang University, 74 Xuefu Road, Harbin 150080, China
[b] Department of Chemistry, Faculty of Science, National University of Singapore, 3 Science Drive 3, Singapore 117543, Singapore
[c] Institute of Materials Research and Engineering, Agency for Science, Technology and Research, 3 Research Link, Singapore 117602, Singapore

Contents

Abbreviations: Alq_3, tris(8-quinolinolato) aluminum(III); AFTFBD, 2-acetylfluorene-4,4,4-trifluorobutane-1,3-dione; BCP, 2,9-dimethyl-4,7-diphenyl-1,10-phenanthroline; BFPP, 2,3-bis(4-fluorophenyl)pyrazino[2,3-f] [1,10]phenanthroline; bpy, bipyridine; Bphen, 4,7-diphenyl-1, 10-phenanthroline; BTA, 4,4,4-trifluoro-1-phenyl-butane-1,3-dione; CBP, 4,4′-bis(9-carbazolyl)-2,2′-biphenyl; CE, current efficiency; CIE, Commission internationale de L′Eclairage; CPIP, 5-(5-carboxylatopyridin-2-yl)isophthalate; CRT, cathode ray tube; CT, charge transfer; CTL, carrier transporting layer; CV, cyclic voltammetry; D–A–A, donor–acceptor–acceptor; DBM, 1,3-diphenylpropane-1,3-dione; DCJTB, 4-(dicyanomethylene)-2-t-butyl-6-(1,1,7,7-tetra methyljulolidyl-9-enyl)-4H-pyran; DF, 4,5-diazafluorene; DPA, diphenylamine; DPEPO, bis(2-(diphenylphosphino)phenyl) ether oxide; DPPZ, 4,5,9,14-tetraazabenzotriphenylene; DPDBM, 1-(4-diphenylamino-phenyl)-3-phenyl-propane-1,3-dione; EFDPO, (9,9-diethyl-9H-fluorene-2,7-diyl)bis (diphenylphosphine)oxide; EL, electroluminescent; EMLs, emissive layer; EPIP, 3-ethyl-2-phenylimidazo [4,5-f] 1,10-phenanthroline; EQE, external quantum efficiency; ET, energy transfer; ETL, electron-transport layer; FDPO, 9,9-bis(diphenylphosphorylphenyl)fluorene; FMOs, frontier molecular orbitals; FRET, Förster resonance energy transfer; FWHM, full width at half maximum; HDLCD, high-definition liquid crystal display; HIL, hole-injecting layer; HOMO, highest occupied molecular orbital; HPIP, 2-phenylimidazo [4,5-f]1,10-phenanthroline; HTL, hole-transporting layer; IC, internal conversion; IET, intramolecular energy transfer; IP, imidazole fused phen; ISC, intersystem crossing; ITO, indium tin oxide; LMET, ligand-to-metal energy transfer; LMCT, ligand-to-metal charge transfer; LUMO, lowest unoccupied molecular orbital; MA, maleic acid; MMA, methyl methacrylate; m-MTDATA, 4,4′,4″-tris(3-methylphenylphenylamino)-triphenylamine; NPB, *N*,*N*′-bis-(1-naphthyl)-*N*,*N*′-bipheny-1,1′-biphe nyl-4,4′-diamine; NTA, nitrilotriacetate; Obpy, 2,2′-bipyridine mono *N*-oxide; OLED, organic light-emitting diode; Opy, pyridine *N*-oxide; OXD, 1,3,4-oxadiazole; PBD, 2-(4-biphenylyl)-5-(4-tert-butylphenyl-1,3,4-ox adiazole); PCzPIP, 2-phenyl-3-[3-(carbazol-9-yl)propyl]imidazo [4,5-f]1, 10-phenanthroline; PE, power efficiency; PEDOT:PSS, poly(3,4-ethylenedioxythiophene): poly(styrenesulfonate); PF, polyfluorene; PFO, poly(9,9-dioctylfluorene); Phen, 1,10-phenanthroline; PL, photoluminescence; PLED, polymeric light-emitting diode; PLQE, photoluminescent quantum efficiency; PMMA, poly(methyl methacrylate); PMIP, tris(1-phenyl-3-methyl-4-isobutyryl-5-pyrazolone)(phenanthroline); PO, phosphine oxide; PVK, polyvinylcarbazole; PyBM, 2-prydinyl-benzimidazole; PyPhen, pyrazino[2,3-f][1,10]phenanthroline; sbf, 5-diaza-9,9′-spirobifluorene; TCPD, 1-[3,4,5-tris[4-(9H-carbazol-9-yl)butoxy] phenyl]-3-phenylpropane-1,3-dione; T_d, decomposition temperature; TEM, transmission electron microscope; T_g, glass transition temperature; THF, tetrahydrofuran; T_m, melting point temperature; TOPO, trioctylphosphine oxide; TPA, triphenylamine; TPBI, 1,3,5-tri(1-phenyl-1H-benzo[d] imidazole-2-yl)phenyl; TPD, tri-methylphenyl diamine; TPPO, triphenylphosphine oxide; TPTZ, 2,4,6-tripyridyltriazine; TTA, 2-thenoyltrifluoroacetonate.

* Corresponding author. Tel.: +86 0451 86604764.
** Corresponding author at: Department of Chemistry, Faculty of Science, National University of Singapore, 3 Science Drive 3, Singapore 117543, Singapore. Tel.: +65 6516 1352; fax: +65 6779 1691.
E-mail addresses: hxu@hlju.edu.cn (H. Xu), chmlx@nus.edu.sg (X. Liu).

http://dx.doi.org/10.1016/j.ccr.2015.02.018

ARTICLE INFO

Article history:
Received 20 October 2014
Received in revised form 22 February 2015
Accepted 24 February 2015
Available online 6 March 2015

Keywords:
Electroluminescence
Europium complex
Lanthanide
Energy transfer

ABSTRACT

Lanthanide complexes are widely used as emitters for applications in the fields of bioimaging, molecular sensing, disease diagnosis, and optoelectronics. Particularly, the high luminescence efficiencies of these complexes make them attractive for electroluminescent display and solid-state lighting. As color purity and saturation are the most stringent criteria for red emission in display technology, europium(III) complexes featuring an emission peak centered at ~612 nm with a narrow bandwidth hold great potential as red-emitting materials. This review highlights the recent development of electroluminescent europium(III) complexes, with emphasis on correlations between molecular structures and optoelectronic performance. After a fundamental introduction on the optical and electrical properties of europium(III) complexes, efforts will be devoted toward the controlled synthesis and functionalization of molecules for improved charge injection/transportation, good processability, and enhanced emission efficiency.

1. Introduction

The choice of the emitters incorporated in the emissive layer (EML) of organic light-emitting diodes (OLEDs) dictates many photophysical processes, such as emission color tuning, photodegradation, radiative energy transition, as well as electrical modulation of the devices [1–3]. For example, the frontier molecular orbital (FMO) energy gap between an emitter and the charge-carrier transporting material deposited in adjacent layers directly determines the drive voltage of the device. In recent years, driven by pressing demands for lighting products, displays and other commercial applications, much research effort has centered on improving electroluminescent (EL) efficiencies and device stability. With these concerns in mind, researchers extensively investigate purely organic dyes and transition-metal complexes owing to their suitability as emitters for optoelectronic modulation. Nevertheless, in view of complex electronic transitions, the emission spectra of organic dyes and transition-metal complexes are asymmetric and broad with a large full width at half maximum (FWHM) of more than 3000 cm^{-1}. This precludes the use of these molecules to achieve high-definition display where high color purity and narrow emission band are essential [4–6].

Luminescent complexes comprising lanthanides are known as the emitters with high color purity owing to the characteristic *f–f* transitions of the lanthanides [7–13]. In most cases, lanthanide complexes have narrow emission bandwidths with FWHM smaller than 100 cm^{-1}, making possible the so-called monochromic emission. Therefore, lanthanide-based phosphors were often employed in video display terminals with high color saturation, such as cathode ray tube (CRT) and high-definition liquid crystal display (HDLCD) [14,15]. Fig. 1a shows the spectroscopic components of white emission from a commercial Lenovo ThinkVision™ L197 LCD display in which three primary colors were attributed to $^1G_4 \rightarrow {}^3H_6$ transition of Tm^{3+} for blue at ~430 nm, $^5D_4 \rightarrow {}^7F_5$ transition of Tb^{3+} for green at ~545 nm and $^5D_0 \rightarrow {}^7F_2$ transition of Eu^{3+} for red at ~612 nm. Therefore, one would intuitively expect the prospect of developing lanthanide organic phosphors for OLED applications.

In terms of OLED performance with high color purity in red emission, EL Eu^{3+} complexes present an unique opportunity as red-emitters for those striving for advanced technology solutions. In favor of inorganic Eu^{3+} emitters with comparable $^5D_0 \rightarrow {}^7F_J$ transition intensities ($J = 1$ and 2), Eu^{3+} complexes provide an asymmetrical ligand field that drastically facilitates the $^5D_0 \rightarrow {}^7F_2$ transition to yield an essentially monochromic single-band red emission at 612 nm (Fig. 1b). For common organic compounds, the generation of red emission typically requires a FMO energy gap of less than 2.0 eV, which is apparently too small for realizing energy level matching with adjacent charge transfer layers (CTLs). However, the matching of the energy levels with CTLs is feasible in Eu^{3+} complexes because their FMO energy gaps can be precisely controlled by ligand modification and functionalization. Owing to the highly localized emission nature of Eu^{3+}, moderate ligand conjugation and functionalization would not influence emission color purity of the resulting complex, thus allowing for convenient molecular design and integration of multiple functions. Since both singlet and triplet excitons can be harvested during EL processes, it is believed that the theoretical internal quantum efficiency of the devices made of Eu^{3+} complexes can approach to 100% [16].

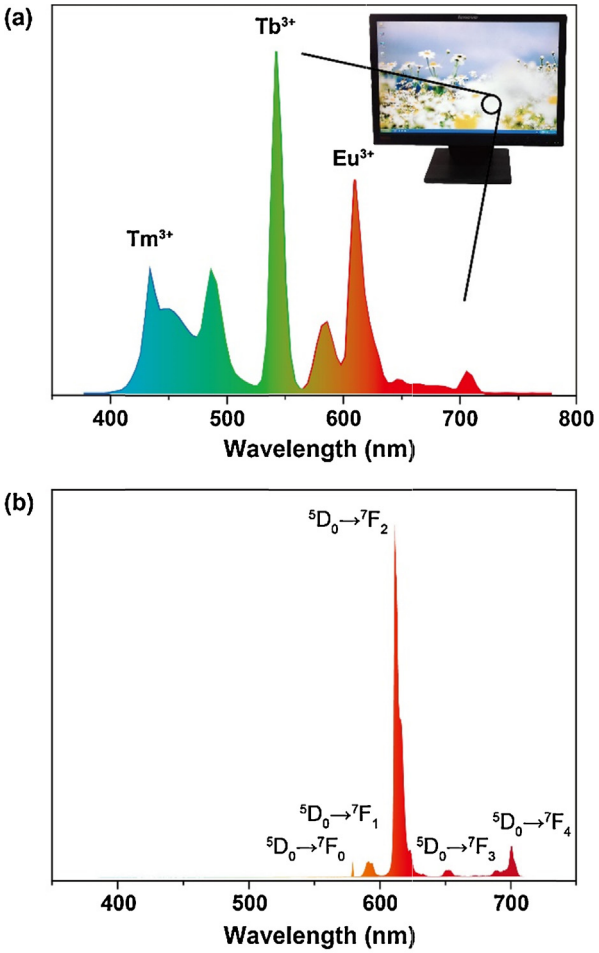

Fig. 1. (a) Emission spectrum of white-light area of Lenovo ThinkVision™ L197 display, recorded with a PR-655 Spectra Colorimeter at 150 cd m^{-2}; (b) typical photoluminescence spectrum of organic Eu^{3+} complexes.

In this article, the importance of Eu^{3+} complexes as EL materials for optoelectronic applications is reviewed. An overview describing

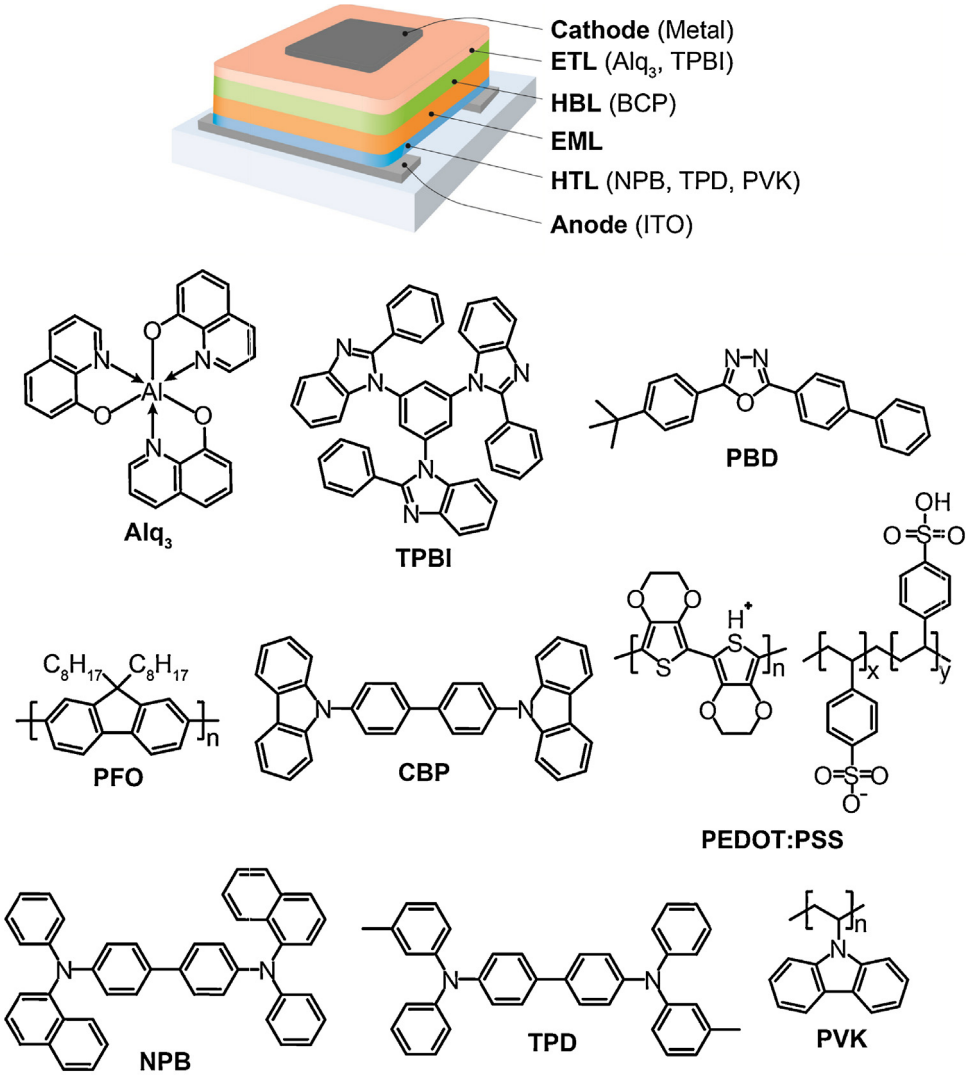

Fig. 2. Typical OLED structures and chemical structures of organic molecules commonly used for OLEDs. ETL: electron-transporting layer; HBL: hole blocking layers; EML: emissive layer; HTL: hole-transporting layer.

the basic principles for designing bright and efficient Eu^{3+} complexes will first be introduced. We will then focus on the Eu^{3+} complexes comprising small molecules, polymers, and nanoscale structures. The emphasis will be placed on ligand functionalization and the establishment of complex systems. In addition, the universal physical and chemical effects of Eu^{3+} complexes on EL processes will be highlighted. This review seeks to provide perspectives on innovative design strategies, feasible modification approaches, fundamental challenges and future directions for EL Eu^{3+} complexes.

2. Basic operating principles of EL Eu^{3+} complexes

2.1. Device structure consideration

An OLED is typically composed of thin organic layers in which emitters and host matrices are sandwiched between two electrodes (Fig. 2) [17]. Owing to weak electroactivity of Eu^{3+} complexes, functional layers are commonly employed to assist charge injection, transport and blocking for improved device performance. When DC current is applied, charge carriers from the anode and cathode are injected into the organic layers. Visible light is emitted as a result of electroluminescence. In view of the number of organic layers used, device configuration can be divided into monolayer, bilayer, trilayer, and tetralayer structures, *etc*. For devices grown by vacuum thermal evaporation, CBP is the most popular host matrix displaying excellent ambipolar characteristics, while NPB and TPD are used as the hole-transporting layer. Additionally, Alq_3 and TPBI serve as the electron-transporting layer, and BCP is commonly incorporated as the hole-blocking layer. For spin-coated devices, PVK and PFO are employed in combination with electron-transporting PBD as host matrices, while PEDOT:PSS and PVK are utilized as the hole-injecting and hole-transporting layer, respectively.

The OLED's optoelectric characteristics are measured by three basic parameters: drive voltage, current density and luminance, expressed in SI units of volt (V), milliampere per square centimeter ($mA\,cm^{-2}$), and candela per square meter ($cd\,m^{-2}$), respectively. The threshold voltage at a luminance of $1\,cd\,m^{-2}$ is commonly defined as turn-on voltage (V_{on}). For computer screens and fluorescent lamps, 100 and $1000\,cd\,m^{-2}$ are regarded as suitable levels of luminance for practical display and lighting, respectively. The electro-optical conversion efficiency of OLEDs are determined by current efficiency (CE, η_A), power efficiency (PE, η_P) and external quantum efficiency (EQE, η_E), which are defined as the ratios of luminosity to current, luminous to electrical power, and the photons out of the device to the number of injected electrons, respectively. Notably, the EL spectra of OLEDs are generally too

broad to be treated as a monochromatic light source, and an averaged value of photon energy is taken for calculation. As a result, the use of a single value of photon energy is intrinsically not reliable for representing a broad light emission distribution.

$$\eta_A = \frac{L \times A}{I} \quad (1)$$

$$\eta_P = \frac{L_P}{I \times V} \quad (2)$$

$$\eta_E = \frac{N_P}{N_C} \quad (3)$$

where L is the luminance, A is the emissive area, I is the current, L_P refers to luminous power calculated by the equation of $L_P = \pi \times L$ for a unilateral planar excitation source, V is voltage, N_P and N_C refer to the respective numbers of photons and hole–electron pairs.

2.2. Intramolecular energy transfer in Eu^{3+} complexes

The electronic transitions of lanthanide ions are forbidden by parity selection rules, leading to weak absorbance. To overcome the intrinsically low molar absorption coefficients of lanthanide ions, a sensitization process involving the population of the excited state of the lanthanide ions *via* energy transfer from an organic antenna chromophore is generally employed. The emission of these lanthanide complexes usually takes place *via* a three-step process: ligand excitation, energy transfer (ET) from the ligand to the lanthanide, and deactivation of the excited lanthanide. The apparent photoluminescent quantum efficiency (PLQE, Φ) can be expressed as:

$$\Phi = \Phi_L \cdot \Phi_{ET} \cdot \Phi_{Ln} \quad (4)$$

where Φ_L is the internal quantum efficiency of the ligand, Φ_{ET} refers to ET efficiency from the ligand to lanthanide, while Φ_{Ln} is radiative efficiency of the lanthanide. Since Φ_{Ln} is a constant for a given lanthanide ion, optical properties related to the sensitizability and excited energy level of the organic ligand are crucial to emissive performance of the resultant complex. Furthermore, as spontaneous emission probability of lanthanide ions can be improved by the ligand field effect as discussed in Section 2.2, the intrinsic limitation of PLQE for Ln^{3+} can be overcome, giving rise to almost 100% PLQE for quite a few Eu^{3+} complexes.

The intramolecular energy transfer (IET) process in typical binary systems consisting of anionic ligands and lanthanide ions was well established by Weissman [18], Dexter [19], Crosby [20] et al., who proposed three fundamental mechanisms: (i) The first mechanism involves ligand excitation to its singlet excited level, then optical transition to the first singlet excited level (S_1) through internal conversion (IC), followed by energy transfer to $^5D_0$ or higher excited levels of Eu^{3+}; (ii) Different from the first situation, an intersystem crossing process is likely to be involved by energy transfer from S_1 to triplet excited energy levels, followed by a rapid IC process to reach to T_1. Energy is transferred to excited Eu^{3+} from the triplet levels; (iii) For the third mechanism, both singlet and triplet ET processes may occur by mixing the direct energy transfer from singlet levels to higher excited levels of Eu^{3+}. It is important to note that ligand triplet states should be utilized in the emission process of lanthanide complexes as evident by their long emission lifetimes in the range of microseconds or milliseconds [21]. Actually, triplet levels of ligands are typically involved in the IET process for improved ET efficiency by reducing IC-mediated energy loss. The metal complex displays the highest PLQE if the energy is transferred from the lowest triplet excited level of the ligand directly to $^5D_0$ of Eu^{3+} (17,267 cm^{-1}), with the optimal energy gap between T_1 and $^5D_0$ in the range of 2500–5500 cm^{-1} according to Latva's empirical rule [22].

For ternary systems, both neutral and anionic ligands can serve as the antenna to harvest and transfer energy to Ln^{3+}. Therefore, ternary complexes are superior in property modulation through rational function integration and complementation of neutral and anion ligands, such as wide-band absorption and electroactivity. Different with binary analogs, both ligand-to-lanthanide and ligand singlet-to-ligand triplet ET processes should be considered (Fig. 3). Commonly, an anionic ligand is chosen with suitable T_1 to meet Latva's empirical rule, while a neutral ligand should possess suitable excited levels to support ET to the anionic ligand and Ln^{3+}. Huang and co-workers demonstrated that a reverse triplet ET from an anionic to neutral ligand can occur when the T_1 level of the neutral ligand is lower than that of the anionic ligand, thus leading to significant reduction in energy conversion efficiency [23]. Therefore, a typical energy transfer process in ternary Eu^{3+} complex should include two parts: $^{NL}S_1 \rightarrow {}^{AL}S_1 \rightarrow {}^{AL}T_1 \rightarrow {}^5D_0$ and $^{NL}S_1 \rightarrow {}^{NL}T_1 \rightarrow {}^{AL}T_1 \rightarrow {}^5D_0$ (NL and AL refer to neutral and anionic ligand, respectively.) With time-resolved spectroscopic investigations, Xu et al. showed that when the T_1 level of the neutral ligand is located between the S_1 and T_1 levels of the anionic ligand, the transfer of energy can proceed from the S_1 state of the neutral ligand to the $^5D_0$ state of Eu^{3+} through a stepwise process: $^{NL}S_1 \rightarrow {}^{NL}T_1 \rightarrow {}^{AL}S_1 \rightarrow {}^{AL}T_1 \rightarrow {}^5D_0$ [24]. The involvement of $^{NL}T_1 \rightarrow {}^{AL}S_1$ inter-ligand ISC process remarkably reduces energy loss caused by IC and vibrational relaxation. Therefore, the realization of efficient energy transfer between the neutral and anionic

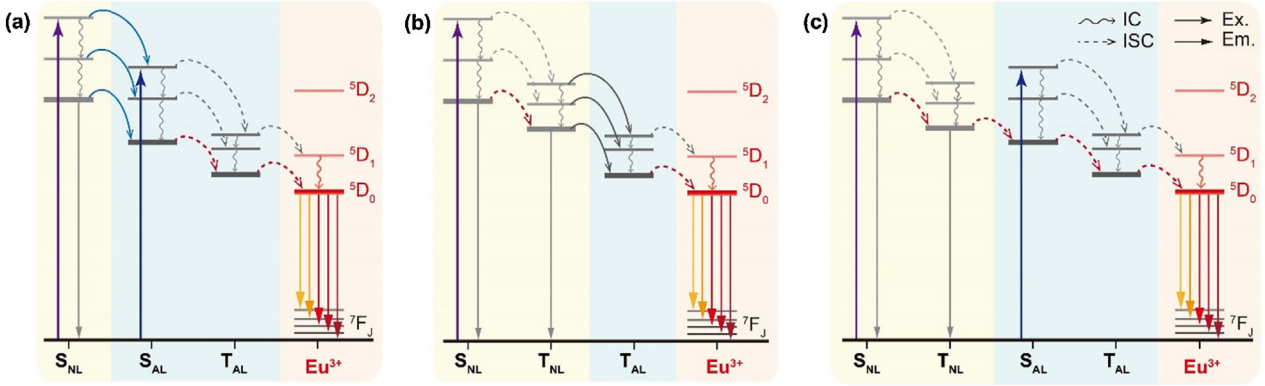

Fig. 3. Jablonski energy level diagram showing principal luminescence processes of (a) $^{NL}S_1 \rightarrow {}^{AL}S_1 \rightarrow {}^{AL}T_1 \rightarrow {}^5D_0$, (b) $^{NL}S_1 \rightarrow {}^{NL}T_1 \rightarrow {}^{AL}T_1 \rightarrow {}^5D_0$, and (c) $^{NL}S_1 \rightarrow {}^{NL}T_1 \rightarrow {}^{AL}S_1 \rightarrow {}^{AL}T_1 \rightarrow {}^5D_0$ in a ternary Eu^{3+} complex. (NL: neutral ligand; AL: anion ligand; IC: internal conversion; ISC: intersystem crossing; Ex: excitation; Em: emission).

ligand in ternary lanthanide complexes is a crucial research subject for achieving high performance of optoelectronic devices.

2.3. Molecular design strategy for EL Eu^{3+} complexes

The molecular design of EL Eu^{3+} complexes as emitters is mainly oriented toward enhancement of optical performance with simultaneous consideration of electrical modification and improvement of processability.

2.3.1. Energy level compatibility

With an increased organic proportion in a ternary Eu^{3+} complex, the enhancement in energy harvesting ability actually plays second fiddle. The main attention is concentrated on the modulation and matching of energy levels. Considering the requirement of direct energy transfer from T_1 of ligand to $^5D_0$ of Eu^{3+}, anionic ligands with suitable T_1 levels are generally selected prior to the selection and construction of neutral ligands in order to realize an efficient intramolecular energy transfer in addition to the ligand-to-Eu^{3+} energy transfer.

2.3.2. Ligand field effect

Judd–Ofelt theory shows the significant influence of a ligand field on luminescent performance of Ln^{3+} complexes, which is actually a combined result of crystal field effects, coordination strength and distance, steric shielding effects toward quenching, *etc.* [25]. These influencing factors are largely determined by ligand structures, *e.g.* symmetry, coordination anchor site, molecular volume and configuration.

2.3.3. Electrical performance

For electroluminescence applications, facile and balanced charge injection and transportation form the basis that influences the exciton recombination and refinement on Eu^{3+} complexes. Thus, the incorporation of carrier-transporting groups is often utilized to improve electroactivity of the complexes.

2.3.4. Processability

Ternary Eu^{3+} complexes often suffer from poor processability for the following two reasons. The weak strength of the coordination bond, formed especially between a neutral ligand and Eu^{3+}, can result in decomposition of the complex during vacuum evaporation. Secondly, considering ligand-Eu^{3+} ET efficiency, most of the complexes employ bidentate ligands to form chelate structures, which reduce the solubility and solution-processability. To this end, ligands that can provide stable coordination to Eu^{3+} and solubilizing groups need to be developed.

It is obvious that contradictions exist between the proposed strategies for molecular modification. For example, since carrier-transporting groups are generally conjugated, the involvement of these groups for improving electroactivity is likely to markedly alter the excited energy levels, thereby leading to energy level mismatch. The challenge in molecular design remains as to how one can effectively integrate various functionalities while concurrently mitigating the negative impacts of different groups.

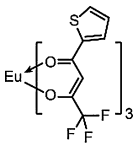

1: $Eu(TTA)_3$

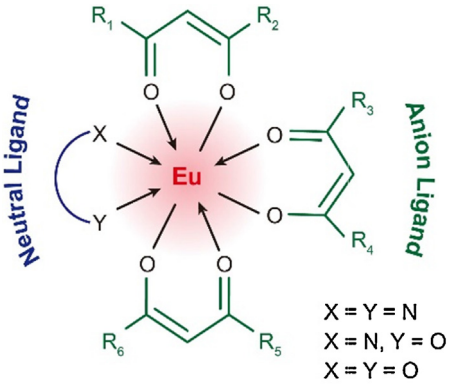

Fig. 4. Chemical structures of typical ternary β-diketonate Eu^{3+} complexes.

3. Electroluminescent Eu^{3+} complexes

The 8-to-10 coordination sites of Eu^{3+} ion can be occupied by three bidentate anionic ligands and one or two neutral ligands to form binary or ternary structures. In contrast to the first report on electroluminescence from a binary Eu^{3+} complex $Eu(TTA)_3$ (**1**, TTA: 2-thenoyltrifluoroacetonate) [26,27], most of EL Eu^{3+} complexes now adopt a ternary configuration between the central metal ion, anionic and neutral ligands by taking advantage of superiority in ligand-to-Eu^{3+} ET efficiency and device integration. In this layout, bidentate anionic ligands typically feature one negative and one neutral coordination sites involving oxygen because of its strong coordination ability to Ln^{3+}. The remaining coordination number can be saturated with four monodentate or two bidentate neutral ligands with either nitrogen or oxygen moiety. Typical examples of 8-coordinated EL Eu^{3+} complexes based on β-diketonate as the ligand were depicted in Fig. 4.

The modification on EL Eu^{3+} complexes is performed by the functionalization of anionic ligands, neutral ligands or both with emphasis on energy level regulation, electrical performance enhancement, and processability improvement. In the following section, the progress of EL Eu^{3+} complexes is discussed in detail with the classification according to ligand functionalization, material type and EL mechanism investigation.

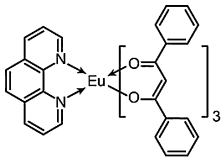

2: $Eu(DBM)_3Phen$

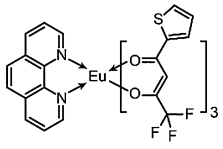

3: $Eu(TTA)_3Phen$

3.1. Anionic carrier-transporting ligands

Since the pioneer work by Kido et al. in 1994 [28], who reported a typical ternary Eu^{3+} complex $Eu(DBM)_3Phen$ (**2**, DBM: 1,3-diphenylpropane-1,3-dione and Phen: 1,10-phenanthroline) with a maximum brightness of 460 cd m^{-2}, β-diketonate and its derivative have become the most popular anionic ligands for preparing EL Eu^{3+} complexes because of their strong sensitizing ability and suitable S_1 and T_1 excited energy levels for efficient IET to Eu^{3+} ion. Another popular anion ligand is β-diketonate TTA molecule that can supply its Eu^{3+} complex in combination with 1,10-phenanthroline, $Eu(TTA)_3Phen$ (**3**), with a maximum brightness of about 140 cd m^{-2} [29].

It is important to note that the low electroactivity of Eu^{3+} complexes is one of the drawbacks associated with their unsatisfied EL performance, such as high drive voltages and low efficiencies. An effective solution to enhance electrical properties is to incorporate

functional groups, such as arylamine and heterocyclic rings with strong electron-donating and electron-withdrawing effects for hole and electron injection and transportation, respectively.

Carbazole is one of the most popular hole-transporting groups with low ionization potential and good host characteristics. Bazan and co-workers first introduced the carbazole with hexyloxyl functional group into β-diketonate for enhanced hole transportation and improved solution processability [30]. The resulting complex **4** showed an impressive PLQE of 50% from its high-quality thin film casted by spin coating. The improvement in electrical properties was supported by the reduction in the energy gap (calc. 2.71 eV) between highest occupied molecular orbital (HOMO) and lowest unoccupied molecular orbital (LUMO). As a result, a bilayer spin-coated device of ITO/PVK/**4**/Ca realized a brightness of 50 cd m^{-2} and an EQE of 0.3%.

Gong and co-workers employed carbazole instead of phenyl in 4,4,4-trifluoro-1-phenyl-butane-1,3-dione (BTA) to form 2-TFDBC and its Eu^{3+} complex **5**, while a dinuclear analog **6** was prepared by incorporating two β-diketonate units at the 2- and 7-positions of carbazole [31]. The red emission with high color purity was observed with Commission internationale de L'Eclairage (CIE) coordinates of (0.68, 0.32). The conjugation extends the Eu^{3+}-sensitized absorption to the blue range. The **5**-doped film showed a relatively high PLQE of 28% as opposed to the film containing complex **6** (10%), which can be ascribed to the elevated effect of quenching because of shortened Eu–Eu distance in dinulear structures. The emission performance of the complex was further improved using complex **7** comprising an additional trifluoromethyl group at the **7**-position of carbazole [32]. As a result of suppressed C—H vibration by fluorine substitutions, the PLQE of complex **7** was enhanced to 34%, furnishing its corresponding InGaN chips with bright, pure red emission. By comparison, Complexes **8** and **9** modified with additional methyl and thiophthene groups showed low device efficiencies [33,34].

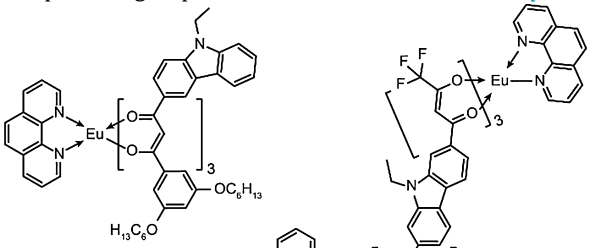

4

6: Eu_2(2,7-BTFDBC)$_3$(Phen)$_2$

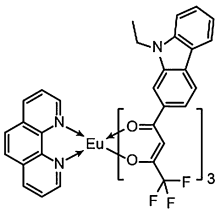

5: Eu(2-TFDBC)$_3$Phen

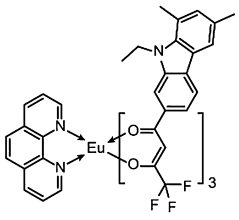

8

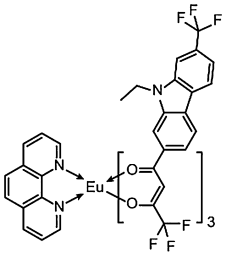

7: Eu(ETFMCTFBD)$_3$Phen

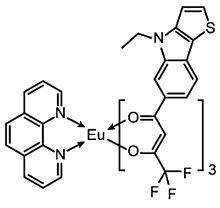

9

Huang and Xie and their co-workers developed a series of carbazole-functionalized Eu^{3+} complexes (**10**–**13**) using a typical Eu^{3+} complex Eu(DBM)$_3$Phen (**2**) as the core, in which peripheral carbazole groups enhance energy harvesting and hole injection/transportation [35,36]. Carbazolyls were linked to β-diketonate *via* *n*-butyl groups to block conjugation extension and limit triplet energy reduction. The PLQE of complexes **10**–**12** is 3–7 times higher than that of carbazole-free complex **13**, suggesting enhanced sensitization and population of Eu^{3+} excitons by carbazoles. By utilizing complex **11** as dopant to fabricate a trilayer device of ITO/NPB/CBP:**11**/BCP/Mg:Ag, a bright white electroluminescence with favorable CIE coordinates of (0.33, 0.35) was realized in which three main emission peaks at 487, 563 and 610 nm can be attributed to the exciplex formation between CBP and carbazole dendrons, the electroplex formation of the TCPD ligand, and $^5D_0 \rightarrow {}^7F_2$ transition of Eu^{3+}, respectively [37]. The white-light-emitting device containing complex **11** achieved a maximum luminance of 229 cd m^{-2}, a power efficiency (PE) of 0.2 lm W^{-1}, and an EQE of 1.1%.

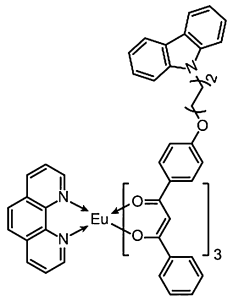

10: Eu(MCPD)$_3$Phen

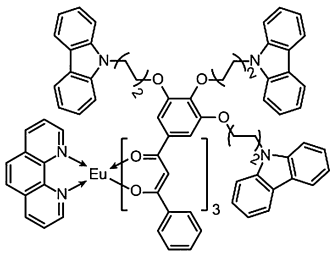

11: Eu(TCPD)$_3$Phen

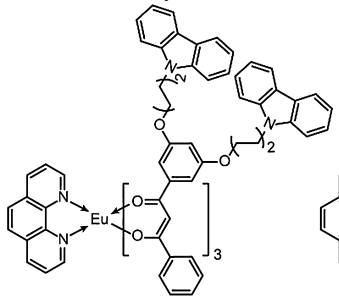

12: Eu(BCPD)$_3$Phen

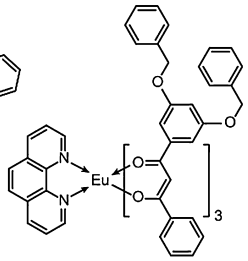

13: Eu(BPPD)$_3$Phen

The strong sensitizability of carbazole group was further demonstrated by Zheng et al. in comparison to DBM and 1,10-phenanthroline groups [38,39]. In DBM-Carb-based complexes **14** and **15**, two carbazole groups were introduced symmetrically at the *para*-position of the two phenyl groups. Although this configuration can effectively reduce the steric hindrance of the anionic ligand, the PLQEs of **14** and **15** were 18 and 14%, respectively. The locally symmetrical ligand field in **14** and **15** rendered their transition probability of $^5D_0 \rightarrow {}^7F_2$ transition of Eu^{3+} smaller than that of unsymmetrical complex **12**, thereby leading to low PLQEs relative to **12**.

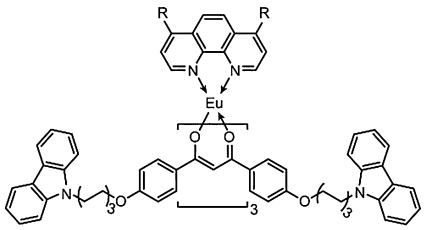

14: R = H Eu(DBM-Carb)$_3$Phen

15: R = Eu(DBM-Carb)$_3$BPhen

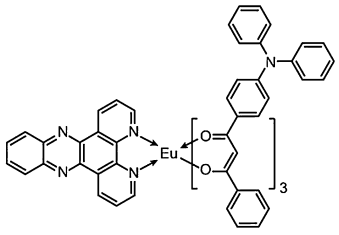

16: Eu(DPDBM)$_3$DPPZ

Under the same consideration, Li and co-workers introduced a hole-transporting diphenylamine (DPA) at the 4-position of one phenyl group in DBM to form an ambipolar Eu^{3+} complex $Eu(DPDBM)_3DPPZ$ (**16**) with 4,5,9,14-tetraazabenzotriphenylene (DPPZ) as electron-transport neutral ligand [40]. The asymmetry of local environment for Eu^{3+} in complex **16** was confirmed by a Ω_2 value of 1.39×10^{-19}, double that of complex **2**. Therefore, although the energy gaps between T_1 levels of DPDBM and DPPZ and $^5D_0$ of Eu^{3+} were too small to prevent reverse energy transfer, complex **16** still achieved a favorable PLQE of 36%. Complex **16** further showed a very short emission lifetime of 30 μs, which is only one tenth of common values for Eu^{3+} complexes. The short emission lifetime is beneficial in suppressing triplet quenching-induced efficiency reduction and roll-offs. Consequently, multilayer devices made of **16** with the configuration of ITO/4,4′,4″-tris(3-methylphenylphenylamino)-triphenylamine (m-MTDATA)/NPB/CBP:**16**/4,7-diphenyl-1,10-phenanthroline(Bphen)/Alq_3/LiF/Al realized a maximum luminance of 2910 cd m^{-2} and a peak CE of 3.0 cd A^{-1}, accompanied with an effectively suppressed roll-off of 13% at a current density of 10 mA cm^{-2}.

Imidazole, pyridine and 1,3,4-oxadiazole (OXD) are typical heterocyclic rings with strong electron-transport ability. Gong and co-workers modified BTA with imidazole and 2,5-diphenyl-1,3,4-oxadiazole to improve sensitizability of the ligands and thermal and luminescent performance of their Eu^{3+} complexes **17**–**19** [41–43]. The conjugation extension by these heterocyclic groups resulted in bathochromic shifts in the absorption spectra of these complexes, accompanied with characteristic Eu^{3+} emission at 612 nm and moderate PLQEs (14–18%). Red-emitting InGaN chips coated with **17** and **19** achieved good color purity with the CIE coordinates of (0.66, 0.33). Notably, complex **17** endowed its light-emitting diode with an improved PE of 0.53 lm W^{-1}. A further effort to achieve ambipolar characteristics was also undertaken by mixing two types of β-diketonates with different electrical properties [44] or integrating two different functional groups with a single β-diketonate component [45]. However, if two different β-diketonates are simultaneously incorporated in an individual molecular complex, controlling the ratio of these diketones in the resulting complexes by coordination reactions becomes challenging. In most cases, the resultant material was actually a mixture of various complexes with different ratios of two β-diketonates. In the case of adoption of bifunctional β-diketonates, the intramolecular charge transfer between donor and acceptor groups should be suppressed to maintain a suitable excited level of the ligand for efficient IET to Eu^{3+}.

To tune conjugation length, molecular rigidity, and electron-transport ability, Shi et al. utilized three different ligands (marked as L1, L2, and L3 in complexes **20**–**22**) by incorporating pyrazole into the skeleton of β-diketonate [46]. Both L1 and L2 ligands possess a T_1 level of ~19,500 cm^{-1} comparable to the energy levels of $^5D_1$ (~19,000 cm^{-1}) and $^5D_0$ (~17,267 cm^{-1}) of Eu^{3+}, thus enabling a direct and efficient energy transfer from the ligand to Eu^{3+}. In contrast, L3 ligand containing a strong electron-withdrawing cyano moiety exhibited a significant reduction in T_1 level (~18,200 cm^{-1}). Pure red emission from **20**-based device of ITO/NPB/CBP:**20**/BCP/Alq_3/Mg:Ag was recognized with luminance up to 247 cd m^{-2}.

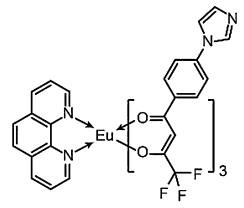

17: Eu(IDTFBD)$_3$Phen

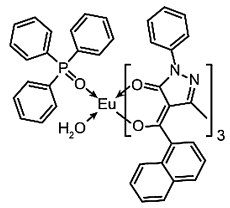

20: Eu(L1)$_3$(TPPO)(H$_2$O)

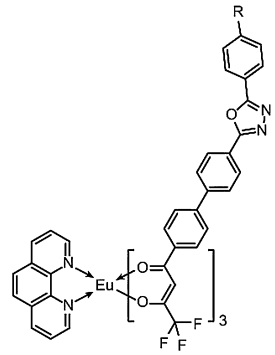

18: R = CH_3 Eu(MPBDTFA)$_3$Phen

19: R = $C(CH_3)_3$ Eu(TPBDTFA)$_3$Phen

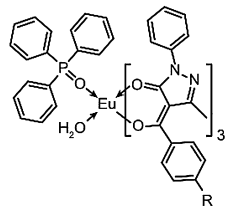

21: R = Eu(L2)$_3$(TPPO)(H$_2$O)

22: R = CN Eu(L3)$_3$(TPPO)(H$_2$O)

As the primary coordinating ligands, anionic ligands exert a crucial influence on optoelectronic properties of their Eu^{3+} complexes. Indeed, this notion forms the basis for constructing brilliant Eu^{3+} complexes. The molecular design of anionic ligands with the aims of adjusting energy levels and enhancing electrical performance has been successfully implemented, leading to the generation of a large variety of red-emitting phosphors with high color purity. However, the critical requirement on excited energy levels and strong coordination stability of the anionic ligands limit their widespread use. To overcome this limitation and broaden topological diversities of metal complexes, a feasible solution is to utilize neutral organic ligands.

3.2. Neutral ligands

The effect of neutral ligands on EL performance enhancement of Eu^{3+} complexes was first identified by Kido's group [27]. The incorporation of 1,10-phenanthroline in ternary complex **3** drastically increased its device brightness to 137 cd m^{-2}, in contrast to less than 1 cd m^{-2} from the device of its binary parent complex **1** [27]. Since anionic ligands play a major role in affording efficient ligand-to-Eu^{3+} energy transfer, the molecular design of neutral ligands is mainly focused on ligand-to-ligand energy level matching and photoelectrical functionalization through conjugation extension and polarity enhancement. The neutral ligands

would serve as the main channel for charge and exciton harvesting. Therefore, despite the minor composition of neutral ligands in complexes, optoelectronic performance of lanthanide complexes is generally dictated by the neutral ligands. According to the different nature of the coordination sites, we divide bidentate neutral ligands into three types, two nitrogen coordination sites (NN̂), one nitrogen and one oxygen coordination site (NÔ), and two oxygen coordination sites (OÔ). In the following section, nitrogen-bearing heterocyclic ligands and aryl phosphine oxides will be discussed.

3.2.1. Nitrogen-bearing heterocyclic ligands

Nitrogen atoms in heterocyclic rings have lone pair electrons to form coordination bonds with empty orbitals of metal ions. Meanwhile, electron-deficient characteristics of conjugated heterocyclic compounds make them competent as electron acceptors for facilitating electron injection and transportation. Therefore, nitrogen-bearing heterocyclic ligands are widely used to construct optoelectronic materials, such as widely used Alq_3 [47]. In Eu^{3+}-based complexes, the involvement of a nitrogen coordination site would enhance asymmetrical ligand field, thus promoting $^5D_0 \rightarrow {}^7F_2$ transition for pure red emission. The planar configurations of most conjugated heterocyclic compounds can also benefit charge transfer (CT) and the confinement of excitons.

3.2.1.1. Phenanthroline derivatives. Zucchi and co-workers reported Eu^{3+} complex **23** with TTA as the anionic ligand and a carbazole-substituted DBM as the neutral ligand [48]. After functionalization, the neutral ligand absorption was broadened with a long tail in the range of 350–400 nm, while the T_1 value of this ligand remained unchanged as ~21,000 cm^{-1} well-suited for efficient ligand-to-metal energy transfer (LMET). The site isolation effect of the modified bulky neutral ligands effectively protects the excited Eu^{3+} from quenching, rendering a monoexponential decay of Eu^{3+} emission with long emission lifetimes (0.66 and 0.80 ms in acetonitrile solutions and films, respectively), along with an impressive high PLQE of 80% in a poly(methyl methacrylate) (PMMA) matrix.

Liu et al. modified 1,10-phenanthroline with two electron-donating triphenylamine (TPA) groups at the 3- and 8-positions to form a neutral ligand DTPA-Phen [49,50]. Its complex **24** showed an extended solid-state absorption with the edge at about 500 nm, overlapping with the emission from a blended host matrix of poly(9,9-dioctylfluorene) (PFO) and *N*,*N*'-bis-(1-naphthyl)-*N*,*N*'-bipheny-1,1′-biphenyl-4,4′-diamine (PBD). This design principle allows for efficient Förster resonance energy transfer (FRET) between the host and the dopant. A moderate PLQE of 12.7% for complex **24** was recorded in degassed DCM solutions. When doped in a matrix of PFO and PBD at a concentration of 1 wt%, complex **24** showed an increased PLQE of 32.7%. Notably, complex **24** exhibited ambipolar characteristics with an elevated HOMO energy level of −5.48 eV and a LUMO energy level of −2.61 eV. With the configurations of ITO/PEDOT:PSS/PVK/PFO:PBD:**24**/Ba/Al, complex **24** endowed its devices with a maximum luminance of 1333 cd m^{-2} and a peak EQE of 1.8%.

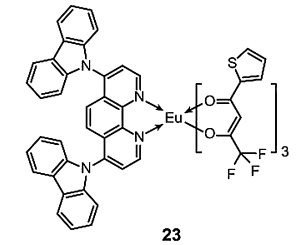

23

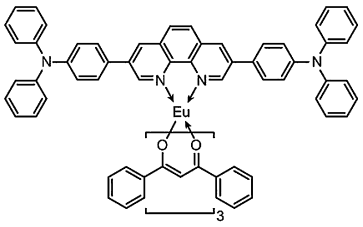

24: $Eu(DBM)_3$(DTPA-Phen)

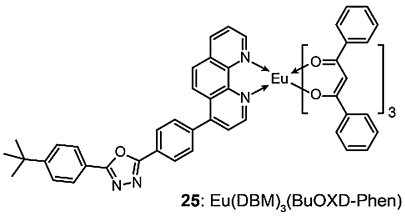

25: $Eu(DBM)_3$(BuOXD-Phen)

Through use of an electron-withdrawing group, Liu et al. synthesized complex **25** by substituting 1,10-phenanthroline with an OXD group at the 5-position [51]. The sensitizability and site isolation effect of complex **25** could be improved by π-electron conjugation or bulky substitution of the OXD group. Furthermore, the strong electron-withdrawing effect of OXD successfully reduced the LUMO level of **25** to −2.72 eV, matching well with the LUMO energy levels of typical electron-transport materials, such as TPBI (1,3,5-tri(1-phenyl-1H-benzo[d]imidazol-2-yl) phenyl; −2.7 eV). The spin-coated device of ITO/PEDOT:PSS/PVK/PFO:PBD:**25**/Ba/Al achieved a maximum luminance of 568 cd m^{-2} and a peak EQE of 1.26%.

In a parallel investigation, Zhu and co-workers simultaneously introduced carbazole and OXD groups in complexes **26**–**34** at the 5-position of 1,10-phenanthroline to afford ambipolar characteristics [52,53]. The ligand-attributed emissions were clearly observed in PL spectra of these complexes dispersed in solutions or deposited as films. Furthermore, the intensities of these ligand emissions were proportional to the volumes of the terminal groups tethered to OXD, suggesting an incomplete LMET process probably caused by steric hindrance. Compared with mononuclear analogs **26**–**30**, PLQEs of complexes **31**–**34** remained essentially the same. It was noticed that the F atom in complex **27** can act as an electron-withdrawing terminal group to reduce the LUMO level of the complex for more than 0.2 eV to facilitate electron injection and transportation, revealing the dominant effect of terminal groups on electrical properties of the complexes. Complex **27** achieved the highest PLQE of 10.5% among these complexes. However, for dinuclear complexes **31**–**34**, the influence of terminal groups became obscure because of their negligible components in the complexes

[53]. The spin-coated devices based on complex **31** with a single-layer configuration of ITO/PEDOT:PSS/PVK:PBD: **31**/LiF/Al showed broadened emissions with a maximum luminance of 48.5 cd m^{-2}. This low brightness should be ascribed to the formation of exciplex and the weak electroactivity of involved long alkyl chain.

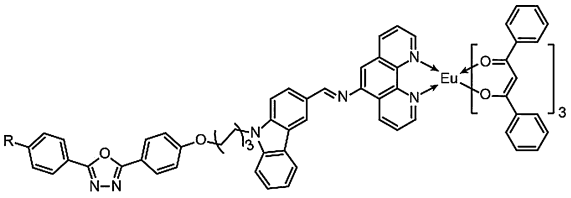

$Eu(DBM)_3RPhOXD_6Cz$-Phen

26: R = H
27: R = F
28: R = Me
29: R = OMe
30: R = ^{t}Bu

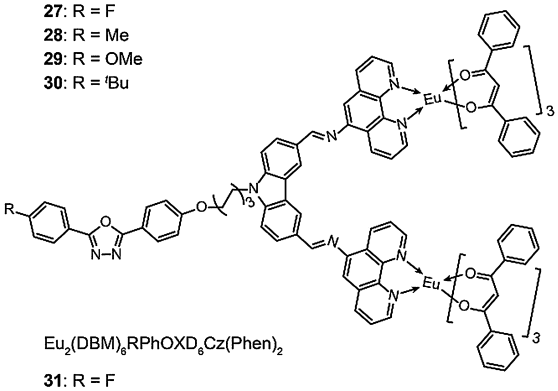

$Eu_2(DBM)_6RPhOXD_6Cz(Phen)_2$

31: R = F
32: R = Me
33: R = OMe
34: R = ^{t}Bu

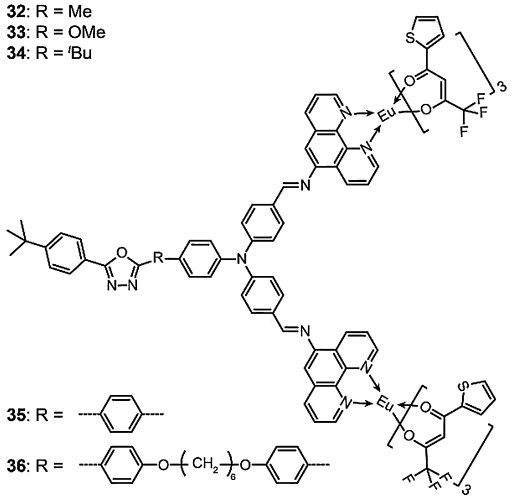

35: R =
36: R =

Similarly, both TPA and OXD were simultaneously employed to construct two ambipolar dinuclear complexes **35** and **36** with phenylene and hexyl linker, respectively [54]. With fully conjugated structure, complex **35** exhibited high thermal stability with a decomposition temperature of 304 °C, which is 52 °C higher than that of complex **36**. Almost a two-fold increase in the PLQE for **35** was obtained relative to **36**. Furthermore, complex **35** was superior to complex **36** in terms of carrier-injection and -transporting abilities. As a result, complex **35** endowed its spin-coated single-layer device with a low turn-on voltage of 8.5 V and a large luminance up to 296 cd m^{-2}.

Cheng and co-workers first developed a series of pyrazino[2,3-f][1,10]phenanthroline (PyPhen) type ligands with high sensitizability and electroactivity for EL Eu^{3+} complexes **37**–**42** [55]. Zhang and co-workers further investigated the optoelectronic properties of these complexes by density functional theory (DFT) simulation. The small-sized ligands can provide more efficient LMET, owing to their higher S_1 and T_1 levels [56]. The involvement of fused pyrazine rings significantly reduced the LUMOs of the complexes to −2.8 to −3.0 eV, giving rise to electron-dominant characteristics and the mechanism of electron-trapping EL [56]. With a device structure of ITO/TPD or NPB/CBP:Eu^{3+} complex/BCP/Alq_3/Mg:Ag, complex **37** endowed its devices with a low turn-on voltage of ~4.7 V, a maximum brightness of 1309 cd m^{-2}, and maximum efficiencies of 1.15%, 2.16 cd A^{-1} and 1.10 lm W^{-1}. Note that DPPZ supported its complex **39** with the best EL performance, including 4.5 V for onset, the maximum luminance of 2046 cd m^{-2}, the peak efficiencies up to 2.05%, 4.38 cd A^{-1} and 2.09 lm W^{-1}. Subsequently, DBM was used to displace TTA in **39** to afford complex **43** [57]. On the basis of a simple bilayer structure in form of ITO/PEDOT:PSS/PVK/PFO:PBD:**43**/Ba/Al, a peak luminance of 1783 cd m^{-2} and maximum efficiencies of 2.5% for EQE and 3.8 cd A^{-1} for CE were realized.

PyPhen was substituted with two fluorophenyls to further enhance electron affinity and site-isolation effect. The resulting ligand BFPP supported its complex **44** with a high PLQE of 55% and a monoexponential decay lifetime of 0.26 ms for Eu^{3+} emission. A maximum luminance of 1766 cd m^{-2} and peak efficiencies of 4.6 cd A^{-1} and 2.27% were achieved through a four-layer device of ITO/TPD/CBP:**44**/Bphen/Alq_3/LiF/Al [58]. Similarly, an indole-fused PyPhen derivative was prepared as the ligand for Eu^{3+}-based complex **45** with a bipolar structure that combines electron-donating indole and electron-withdrawing pyrazine [59].

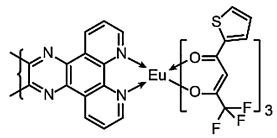

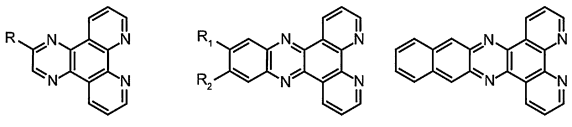

37: R = H PyPhen
38: R = CH_3 MPP
39: R_1 = R_2 = H DPPz
40: R_1 = H, R_2 = CH_3 MDPPz
41: R_1 = R_2 = CH_3 DDPPz
42: BDPz

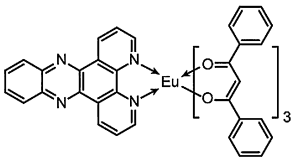

43: $Eu(DBM)_3(DPPz)$

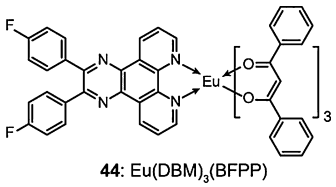

44: $Eu(DBM)_3(BFPP)$

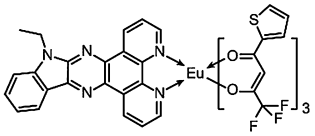

45: $Eu(TTA)_3DIQ$-Et

In 2011, Pereira et al. extended the conjugation of 1,10-phenanthroline by incorporating an electron-deficient five-membered thiadiazole ring to enhance the electron-injection ability of the ligand and its complex **46**. The HOMO and LUMO of **46** were modulated to −5.7 and −2.6 eV, respectively [60]. The Eu^{3+}-originated electroluminescence from a bilayer device of ITO/NPB/CBP:**46**/Al was demonstrated. However, since there was

no substitution position on thiadiazole, this ligand can hardly be functionalized.

Huang and Wang and their co-workers developed a series of imidazole-fused 1,10-phenanthroline (IP) ligands with substitutions at the 1- and 2-positions of the imidazole ring for optoelectronic modulation [61–67]. For example, three ligands, namely HPIP, EPIP and PCzPIP, were prepared by introducing a phenyl group at the 2-position of imidazole and substituting 1-H with ethyl or *N*-propylcarbazole groups [54]. Since the IP group was an electron-deficient ring for electron injection and transportation, the incorporation of hole-transporting carbazole rendered ambipolar characteristics to PCzPIP. All three ligands afforded pure red emissions to their complexes **47**–**49**. In solid state, PL emissions of **48** and **49** were 5 times stronger than that of **47**, in accord with the considerable energy loss associated with a vibrationally excited state of **47**. The bilayer devices of ITO/TPD/**49**/Mg:Ag showed a maximum luminance of 561 cd m^{-2}. This value is more than 150 and 3 times the level of luminance achieved using **47** and **48**, respectively. The enhanced brightness by **49**-based devices should be ascribed to balanced charge fluxes in ambipolar complex **49**. With a trilayer device structure of ITO/TPD/**49**:BCP/BCP/Mg:Ag, the maximum luminance was further improved to 1419 cd m^{-2}, accompanied with a peak PE of 0.88 lm W^{-1}.

In 2009, Zhao and co-workers used complex **50** with a fluorophenyl substituted ligand EFPIP as dopant for the fabrication of a multilayer device comprising ITO/4,4′,4″-tris(3-methylphenylphenylamino)triphenylamine(*m*-MTDATA)/NPB/CBP:**50**/BPhen/Alq_3/LiF/Al [68]. Without an electron-transport layer of BPhen a distinct green emission from Alq_3 can be observed, indicating the low electrical performance of Eu^{3+} complexes. On inserting a 10-nm layer of BPhen in the device, a pure red emission at 612 nm was achieved with CIE coordinates of (0.64, 0.33), a maximum luminance of 465.2 cd m^{-2}, and a peak CE of 3.1 cd A^{-1}.

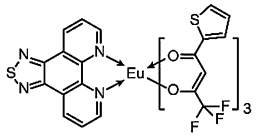

46: $Eu(TTA)_3TDAP$

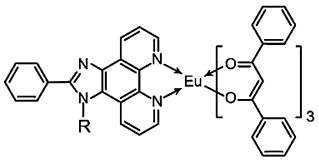

47: R = H $Eu(DBM)_3HPIP$
48: R = C_2H_5 $Eu(DBM)_3EPIP$

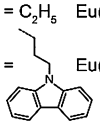

49: R = $Eu(DBM)_3PCzPIP$

With a drastically different approach, Wang and co-workers prepared complexes **51** and **52** by introducing an electron-donating dimethylamine group into the IP ligand in complexes **47** and **48** [62,63]. The improved hole injection and transport in complex **52** was validated by its HTL-absent device (ITO/**52**/Alq_3/Mg:Ag) with 2.5 times improvement in the luminance as compared with its ETL-absent analog (ITO/TPD/**52**/Mg:Ag). When coupled with BCP (ITO/TPD/**52**/BCP/Alq_3/Mg:Ag), complex-**52** based devices showed a luminance enhancement of 230 cd m^{-2} with efficiencies of 0.33 cd A^{-1} and 0.13 lm W^{-1}, respectively.

The same strategy was adopted for constructing two carbazole-modified ligands (Phencarz and CPIP) and their Eu^{3+} complexes **53** and **54** [64–66]. These complexes possessed multi-functional structures with combined use of hole-transport carbazole, electron-transport IP and Eu^{3+}-involved emitting core. PL spectrum of **53** in solution showed emissions from both Phencarz and Eu^{3+}, attributable to solvent-induced structural relaxation in the excited state. In its solid state, only pure red emission was observed. The single-layer devices of **53** showed a luminance of 20 cd m^{-2} and an onset voltage of 7 V, indicating its ability for balanced carrier injection and transport. The **53**-based four-layer devices (ITO/TPD/**53**/BCP/Alq_3/Mg:Ag) achieved a decreased turn-on voltage of 4 V, an improved luminance over 2000 cd m^{-2} at 20 V, and a peak PE of 2.7 lm W^{-1}. However, at voltages greater than 12 V, a distinct emission of Alq_3 was observed. Therefore, instead of Alq_3, tris(1-phenyl-3-methyl-4-isobutyl-5-pyrazolone)-bis(triphenyl phosphine oxide) gadolinium $Gd(PMIP)_3(TPPO)_2$ with LUMO of −3.5 eV was employed as electron-transport layer [65]. The resulting devices emitted pure red light at 612 nm with a maximum luminance of 1193 cd m^{-2} and a PE of 1.68 lm W^{-1}. The bilayer device of ITO/TPD/**54**/Mg:Ag exhibited a low onset voltage of 4 V and a maximum luminance of 537 cd m^{-2}. However, similar to **53**, Alq_3-originated emission was also observed for **54** when adopting a four-layer device configuration with a voltage of higher than 12 V. To increase the maximum luminance and PE of the device, complex **2** was utilized as ETL to prepare a trilayer device composed of ITO/TPD/**54**/**2**/Mg:Ag. The researchers ascribed the improved EL performance of **53** and **54** to an enhanced hole-transporting ability enabled through carbazole modification.

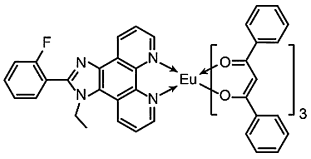

50: $Eu(DBM)_3(EFPIP)$

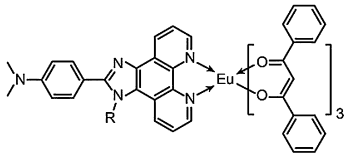

51: R = H $Eu(DBM)_3DMHPIP$
52: R = C_2H_5 $Eu(DBM)_3DMPIP$

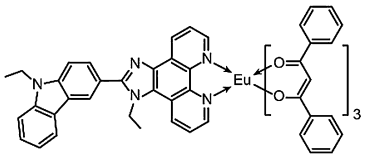

53: $Eu(DBM)_3Phencarz$

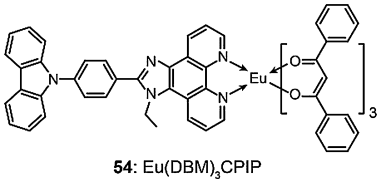

54: $Eu(DBM)_3CPIP$

Alternatively, TPA can be used to facilitate hole injection and transport as demonstrated in complexes **55**–**57** [67,69]. For instance, the Eu^{3+}-originated emission observed in solid-state PL spectrum of complex **55** was in accord with its EL spectra.

The improved double-carrier transporting ability of complex **55** endowed its single-layer devices with a low onset voltage of 8 V and a luminance of 19 cd m^{-2}. In contrast, a four-layer device comprising ITO/TPD/**55**/BCP/Alq_3/Mg:Ag achieved an enhanced luminance of 1305 cd m^{-2} with a reduced turn-on voltage of 6 V, as well as an increased EQE of 0.85% and a PE of 1.44 lm W^{-1}. The electron-transport ability of complex **57** was further enhanced by addition of 1-substituted OXD group [69]. Complex **57** exhibited a short emission lifetime of 160 μs and a comparatively high PLQE of 41%. On the basis of a four-layer device configuration comprising ITO/m-MTDATA/NPB/CBP:Eu^{3+}complex/BPhen/Alq_3/LiF/Al, complex **57** exhibited a maximum luminance of 610 cd m^{-2} and a peak CE of 3.67 cd A^{-1}.

Gong and co-workers prepared a ternary IP ligand EtPOTIP in which TPA, OXD and IP were combined to form a donor–acceptor–acceptor (D–A–A) structure [70]. The resulting Eu^{3+} complex **58** showed high thermal and morphological stability with T_d of 431 °C and T_g of 153 °C. However, in a tetrahydrofuran (THF) solution of complex **58** the authors observed ligand-dominant blue emission, largely related to structural relaxation in the excited states. Nonetheless, in solid state, only Eu^{3+}-dominant emissions were observed with the PLQE approaching 48%.

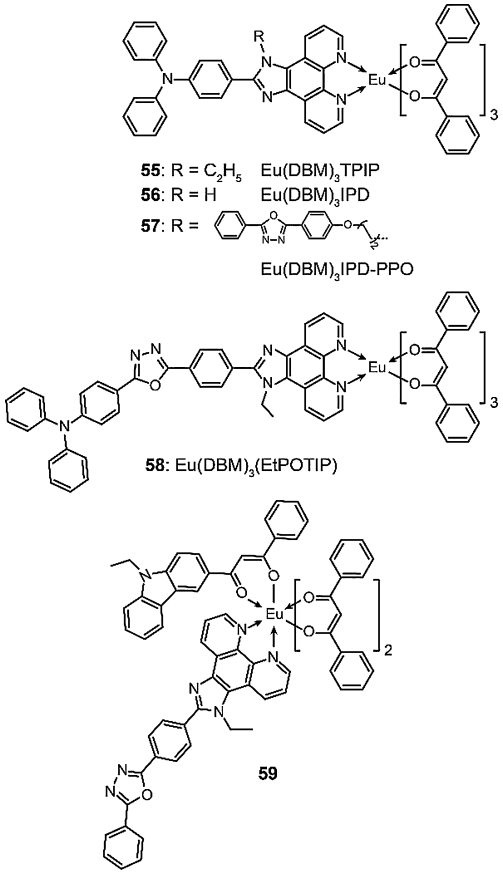

Another strategy to construct ambipolar Eu^{3+} complex was demonstrated by Zhang and co-workers in the case of complex **59**, in which OXD-substituted IP as the neutral ligand and carbazole-modified β-diketonate as the anionic ligand were combined. In this structure, the donor and acceptor groups were separated to achieve suitable excited levels and independent carrier injection and transport, as well as prevent the steric hindrance of each functionalized ligand [71]. Accordingly, the coupling of conjugated carrier-transporting moieties in complex **59** led to appreciable thermal and morphological stability as evident by large T_d and T_g values of 367 °C and 157 °C, respectively. Notably, only pure red emissions originated from Eu^{3+} were observed in the PL spectrum of **59** in solid state, indicating the occurring of an efficient LMET process. The undoped trilayer devices comprising ITO/NPB/**59**/Alq_3/LiF/Al achieved a maximum luminance of 199 cd m^{-2} and a peak CE of 0.69 cd A^{-1}. Encouraged by these results, the researchers further dispersed complex **59** in a CBP matrix and achieved improved device performance, with a luminance of 1845 cd m^{-2}, a CE of 2.62 cd A^{-1}, and a reduced turn-on voltage of 5.5 V.

3.2.1.2. Functionalized bipyridines and analogs. Bipyridine (bpy) is one of the most conventional ligands for preparing luminescent lanthanide complexes with flexible chelate coordination modes and molecular structures [72]. Zheng and co-workers showed that the incorporation of two methoxyls in bpy-type ligands as demonstrated in complexes **60** and **61** can remarkably improve their EL performance [73]. With a doping device configuration comprising ITO/NPB/Eu^{3+} complex:CBP/BCP/Alq_3/LiF/Al, complex **60** realized a maximum brightness of 877 cd m^{-2}, while its maximum CE of 1.19 cd A^{-1} was achieved at a luminance of 3 cd m^{-2}. Complex **61** endowed its device with a maximum brightness of 181 cd m^{-2} and a peak CE of 0.32 cd A^{-1}.

In a parallel study, Huang et al. designed a 2,4-difluorophenyl-substituted bipyridine (DFbpy) as the neutral ligand to enhance the electron-transport ability of complex **62** [74]. The twisting ligand configuration of DFbpy induced by the meso linkage blocks the conjugation between the difuorophenyl and bpy groups, thereby preserving the original excited energy level of bpy in favor of an efficient LMET process. On the basis of a four-layer doping structure (ITO/TPD/CBP:**62**/BCP/Alq_3/LiF/Al), the **62**-based device showed a rather low onset voltage of 5.5 V, a peak brightness of 491 cd m^{-2}, and a PE of 3.2 lm W^{-1}. By utilizing an orange fluorescence dye, 4-(dicyanomethylene)-2-*t*-butyl-6(1,1,7,7-tetramethyljulolidyl-9-enyl)-4H-pyran (DCJTB), as an auxiliary dopant (0.2 wt%) to form an EML, the EL performance of the device comprising CBP:DCJTB:**62** could be further improved, with a maximum luminance of 1200 cd m^{-2} as well as peak efficiencies of 7.3 cd A^{-1} and 2.0 lm W^{-1}. An extremely high CE of 5.8 cd A^{-1} was recorded at a luminance of 100 cd m^{-2} [75].

Pyridine *N*-oxide has high binding affinity for lanthanide ions and strong electron-withdrawing ability to improve electron injection and transport. In 2004, a mono-oxide of bipyridine, namely 2,2′-bipyridine mono *N*-oxide (Obpy), was utilized by Ma and co-workers as the neutral ligand to construct a TTA-based Eu^{3+} complex **63** [76]. The asymmetric configurations of both Obpy and TTA facilitated the parity violation, thereby enhancing the $^5D_0 \rightarrow {}^7F_2$ transition probability of Eu^{3+} for intense pure red emission at 612 nm. With a typical four-layer device structure (ITO/TPD/CBP:**63**/BCP/Alq_3/LiF/Al), complex **63** afforded a maximum luminance of 531 cd m^{-2} and peak efficiencies of 4.6 cd A^{-1}, 2.33 lm W^{-1}, and 2.6%.

On a separate note, You et al. used pyridine *N*-oxide (Opy) as the neutral ligand to prepare a dinuclear Eu^{3+} complex **64** [77]. It was commonly believed that the dinuclear complex would be subject to quenching effects arising from a short Eu^{3+}–Eu^{3+} distance. However, the intermolecular triplet-triplet annihilation was suppressed in complex **64** as two Eu^{3+} ions and two oxygen atoms in pyridine oxide were coplanarly oriented for facile encapsulation of Eu^{3+} ions by the Opy ligand. In consequence, four-layer devices containing **64** showed a maximum brightness of 340 cd m^{-2}, while the efficiencies reached to 2.4 cd A^{-1} and 0.78 lm W^{-1}.

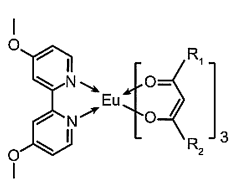

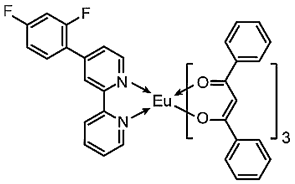

60: R_1 = Ph, R_2 = CF_3 Eu(BTA)$_3$dmbipy
61: R_1 = Th, R_2 = CF_3 Eu(TTA)$_3$dmbipy
62: Eu(DBM)$_3$DFbpy

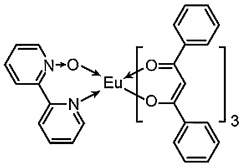

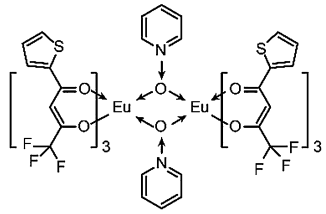

63: Eu(DBM)$_3$Obpy
64: (TTA)$_3$Eu(PyO)$_2$Eu(TTA)$_3$

Compound 4,5-diazafluorene (DF) has more rigid and planar configuration than bipyridine for much improved metal-coordinating ability and high electron injection/transport ability. An intriguing demonstration was demonstrated by Liu et al., who reported two Eu^{3+} complexes **65** and **66** with methoxyl- or OXD-substituted 9,9-diphenyl DF as the neutral ligand, respectively [78]. In contrast to **65**, the sensitizability of OXD groups in **66** made clear by the appearance of additional absorption bands around 310 nm attributable to $\pi \rightarrow \pi^*$ transition of OXD. Both of the complexes gave rise to characteristic Eu^{3+} emissions centering at 612 nm. The bilayer undoped device comprising ITO/TPD/**66**/Mg:Ag achieved a maximum luminance of 154 cd m^{-2} and a peak CE of 0.055 cd A^{-1}, almost four times higher than that obtained by **65**-based devices.

Alternatively, 4,5-diaza-9,9′-spirobifluorene (sbf), a ligand well-known for its good electron affinity, can be employed as the neutral ligand for Eu^{3+} complexation. For example, sbf-based complex **67** showed an intense pure red emission with a high PLQE of 41.23% and a long luminescence lifetime of 1.21 ms [79]. By virtue of the good electron affinity of sbf, the excitons in a trilayer device of ITO/TPD/**67**:CBP/Alq_3/LiF/Al can be efficiently confined in the EML without the need for hole-blocking layer, as evident by the observation of a pure red emission at 100 cd m^{-2}. The device yielded a high maximum luminance of 1365 cd m^{-2} and maximum efficiencies of 5.21 cd A^{-1}, 1.6 lm W^{-1}, and 2.91%.

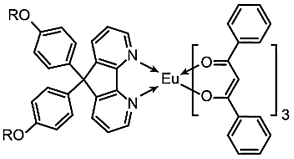

65: R = CH_3 Eu(DBM)$_3$OMe-Spiro-DF
66: R = 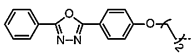 Eu(DBM)$_3$OXD-Spiro-DF

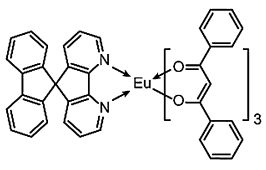

67: Eu(DBM)$_3$(sbf)

3.2.1.3. Benzoheterocyclic ligands. Nitrogen-bearing benzoheterocyclic compounds in which the nitrogen atom may coordinate to metal ions have become an indispensable class of molecules for the preparation of high efficiency EL metal complexes. A common practice of design involves the use of pyridine and its derivatives with substitution groups at the 1-position to construct the benzoheterocyclic ligands. The rigid structure and electron-insufficient characteristics of these ligands are believed to be beneficial for improved electron injection and transport in the resulting metal complexes.

The first report on Eu^{3+}-based complexes comprising neutral ligands modified with benzimidazole was completed by Huang and co-workers in 2001 [80]. The authors constructed complex **68** featuring DBM as the anionic ligand and 2-prydinyl-benzimidazole (PyBM) as the neutral ligand, as well as an ethyl-substituted derivative **69**. A bilayer device of ITO/TPD/**69**/Al realized a maximum brightness of 29 cd m^{-2}. Using a trilayer device configuration of ITO/TPD/**69**/Alq_3/Al, the luminance could be improved to 180 cd m^{-2}. The EL performance of **68** is much worse than that of **69** due to N—H induced vibration energy loss and charge trapping. The researchers solved this problem by substituting N-H in **68** with a long octadecyl group to afford **70**, which showed efficient red emission and improved film formability [81].

One example that clearly shows the importance of facile electron transport for high efficiency device performance was reported by Liang et al., who incorporated OXD into complex **68** through a butyl linker at the 1-position of benzimidazole to form complex **71** [82]. In their work, the OXD absorption was inferred from the appearance of two bands at 311 and 325 nm, while the DBM absorption was shown at a longer wavelength of 349 nm. Owing to the OXD-enhanced electron transport, a bilayer device made of complex **71** with the configuration of ITO/TPD/**71**/LiF/Al showed a maximum brightness of 322 cd m^{-2} and efficiencies up to 1.9 cd A^{-1} and 1.7% at 57 cd m^{-2}.

Li and co-workers introduced a hole-transport carbazole group into the PyBM segment in complex **72** to balance the carrier injection and transport [83]. The voltage-independent saturated red emission at 612 nm with CIE coordinates of (0.67, 0.32) from a trilayer device of ITO/TPD/**72**/TPBI/LiF/Al was verified by a maximum luminance of 200 cd m^{-2} and a maximum CE of 4.2 cd A^{-1}. These results are 3 times higher than those of **68** obtained with the same device configuration.

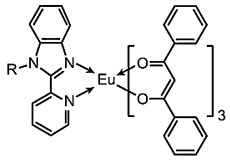

68: R = H Eu(DBM)$_3$HPBM
69: R = C_2H_5 Eu(DBM)$_3$EPBM
70: R = n-$C_{18}H_{37}$ Eu(DBM)$_3$C$_{18}$PBM
71: R = 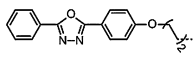 Eu(DBM)$_3$OXD-PyBM
72: R =  Eu(DBM)$_3$CAR-PyBM

Gong and co-workers designed ligands with two and three PyBM units to construct dinuclear and trinuclear complexes **73** and **74**, in which a fluorene-based β-diketonate 2-acetylfluorene-4,4,4-trifluorobutane-1,3-dione (AFTFBD) was utilized as the anionic ligand [84,85]. These complexes have T_d values over 340 °C, indicating the strong coordinating ability of the PyBM moiety to Eu^{3+}. The authors noticed that despite the different stoichiometry of Eu^{3+} in **74** and **73**, the triplet-triplet annihilation effect was not compromised as demonstrated by a high degree of resemblance in their PLQEs, with 15.4 and 16.2% for **73** and **74**, respectively. When embedded in InGaN chips, complex **74** gave rise to a pure

red emission from Eu^{3+} with CIE coordinates of (0.58, 0.29) and a PE of 0.3 lm W^{-1}.

To prevent steric hindrance and possible Eu^{3+}–Eu^{3+} interactions, Su and Wei and their co-workers utilized trimethylene benzene as the core to bridge three PyBM units, resulting in the formation of a flexible ligand TMMB [86,87]. With the TMMB ligand in hand, the authors obtained complex **75** featuring an elongated Eu^{3+}–Eu^{3+} distance. The disrupted π-conjugation in the ligand led to high S_1 and T_1 energy levels, enabling to achieve efficient energy transfer to DBM and then Eu^{3+}. According to cyclic voltammetry (CV) analysis, complex **75** possesses HOMO and LUMO of −5.58 and −3.08 eV, respectively, favorable for charge injection and transport. With a trilayer doping device design (ITO/NPB/CBP:**75**/BCP/LiF/Al), complex **75** showed a pure red emission with CIE coordinate of (0.64, 0.33), a maximum luminance of 109 cd m^{-2}, and a maximum CE of 0.7 cd A^{-1}. Importantly, the EL performance of the trinuclear Eu^{3+} complex is rather modest when compared with their mononuclear analogs. The authors indicate that the poor EL performance of the trinuclear complex is associated with its high molecular weight and low volatility. The compatibility of these molecules with printing methods need to be assessed.

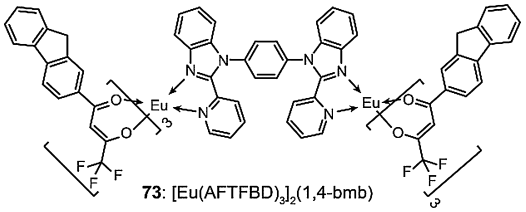

73: $[Eu(AFTFBD)_3]_2$(1,4-bmb)

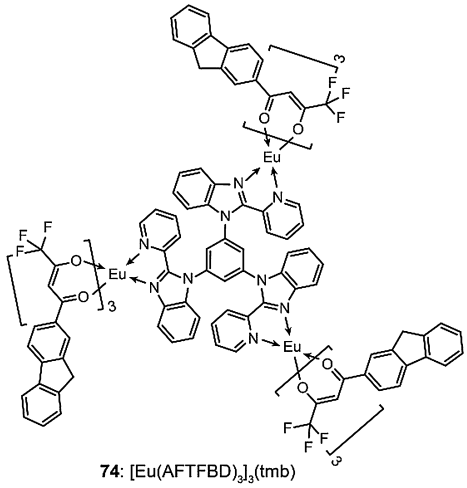

74: $[Eu(AFTFBD)_3]_3$(tmb)

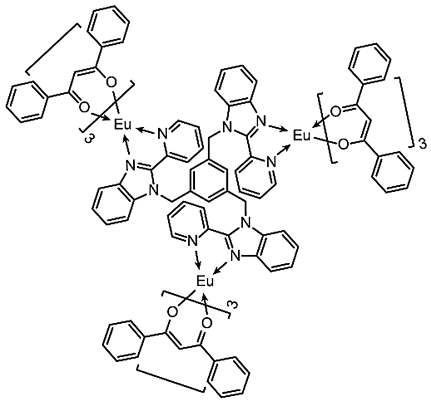

75: $Eu_3(DBM)_3$(TMMB)

In addition to benzimidazole, benzoxazole and benzothiazole molecules with planar configuration and good electron affinity have also been employed to form bidentate neutral ligands, such as PBO and PBT [88]. Their competence as neutral ligands for complexing Eu^{3+} was verified by the observation of pure red emissions from complexes **76** and **77**. Notably, the four-layer devices of **77** (ITO/TPD/Eu^{3+} complex/BCP/Alq_3/Mg:Ag) exhibited a maximum brightness of 148 cd m^{-2} and a maximum current efficiency of 0.08 cd A^{-1}, respectively.

3.2.1.4. Other nitrogen-bearing heterocyclic ligands. Oxadiazole, triazine, pyrazole, triazole and other nitrogen-bearing heterocyclic compounds can be used as building blocks to generate bi- or multidentate ligands. These functional groups allow the formation of metal-complexes with enhanced electron injection and transport and thus improved EL performance.

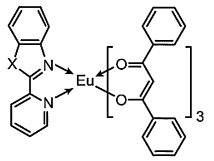

76: X = O Eu(DBM)$_3$PBO
77: X = S Eu(DBM)$_3$PBT

In 2009, Liu et al. incorporated an OXD group at the 2-position of pyridine to form a bidentate ligand as MeO-OXD and its corresponding Eu^{3+} chelate **78** [89]. The similarity in the UV absorption for complexes **78** and **2** revealed a comparable sensitizability of MeO-OXD to 1,10-phenanthroline. When dissolved in chloroform solution or deposited in PVK:PBD blended film, complexes **78** showed pure red emissions at 612 nm, indicating efficient LMET and host-dopant ET processes. A spin-coated single-layer device with the structure of ITO/PEDOT:PSS/PVK:PBD:**78**/Ba/Al was fabricated to generate pure red emission with a maximum luminance of 12 cd m^{-2}.

In 2010, Chen et al. took one step further and prepared a series of tridentate ligands, such as 2-OXD substituted bipyridines and 1,10-phenanthroline derivatives, as well as 2-pyridinyl phenanthroline (Php) for comparison [90]. Complexes **79**–**85** containing these tridentate ligands showed much enhanced thermal stability with T_d in the range of 290–300 °C. The tridentate ligands used for the generation of complexes **79**–**85** provide a coordination number of 9, leading to increased distortion in molecular symmetry and pure red emissions at 612 nm. Owing to their rigid structure and suitable T_1 energy, the phenanthroline-containing ligands furnished their complexes **80**–**82** with PLQE of 30–40%, almost double that achievable by complexes **83**–**85**. With a four-layer **81**-based nondoped device configuration (ITO/TPD/**81**/BCP/Alq_3/Mg:Ag), a maximum luminance of 32 cd m^{-2} was obtained with a broad emission centering at 600 nm. The line-broadening mechanism can be explained by the formation of exciplex between TPD and **81**. When a CBP layer was inserted between the TPD layer and the EML of the four-layer device, the researchers achieved an increased maximum luminance at 67 cd m^{-2}. The low brightness of these nondoped devices is likely due to triplet quenching effects caused by the compact coordination configuration of these tridentate ligands. A distinct increase in the maximum brightness (703 cd m^{-2}) was observed when CBP was used as host material in combination with NPB as hole-transport layer in a four-layer device configuration (ITO/NPB/CBP:**81**/BCP/Alq_3/Mg:Ag), accompanied with increased efficiencies up to 3.0 cd A^{-1} and 0.9 lm W^{-1}.

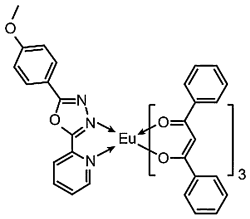

78: $Eu(DBM)_3MeO\text{-}OXD$

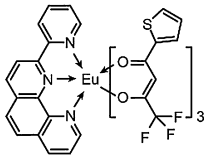

79: $Eu(TTA)_3Php$

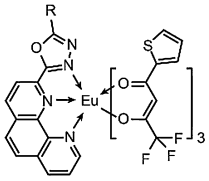

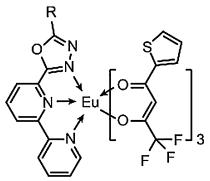

80: R =  $Eu(TTA)_3PhoA$ **83**: $Eu(TTA)_3BpoA$

81: R =  $Eu(TTA)_3PhoB$ **84**: $Eu(TTA)_3BpoB$

82: R =  $Eu(TTA)_3PhoC$ **85**: $Eu(TTA)_3BpoC$

Gusev et al. reported a series of triazole-based bidentate and tetradentate ligands for preparing Eu^{3+}-based complexes **86**–**91** [91–94]. Similar to OXD, triazole is a popular choice for use as electron-transport material. The rigid structure of the triazole ligand provided **88** with high thermal stability (T_d up to 390 °C). All these complexes showed two absorption bands located at 280 and 350 nm, corresponding to absorption by the triazole ligand and DBM, respectively. The asymmetric structure of the triazole ligand facilitates symmetry distortion of it metal complexes in favor of enhanced $^5D_0 \rightarrow {}^7F_2$ transition of Eu^{3+}. Owing to the rigid structure and extended π-conjugation of the triazole ligand, complex **88** exhibited a remarkably high PLQE of 29.1%, almost 5 times the value achievable by **86** and **87**. A trilayer device comprising ITO/NPB/PVK:**89**/Alq_3/LiF/Al yielded a pure red emission with a maximum luminance of ~80 cd m^{-2}.

Several groups have also analyzed the effects of heterocyclic triazine, also known for high electron affinity, on the optical performance of Eu^{3+} complexes **92**–**94** [73,95,96]. The high coordination number of Eu^{3+} in these complexes led to high thermal stability and thus facilitated the $^5D_0 \rightarrow {}^7F_2$ transition of Eu^{3+}, resulting in high PLQEs of 69.7, 40.2 and 15.5% for **92**–**94**, respectively. Four-layer devices made of **92**–**94** with the configuration of ITO/NPB/CBP:Eu^{3+} complex/BCP/Alq_3/LiF/Al showed a characteristic Eu^{3+} emission, accompanied with a weak exciplex emission at 500–600 nm at a high driving voltage. Critically, complex **93** endowed its devices with a maximum luminance of 781 cd m^{-2} and a high CE of 4.76 cd A^{-1} at 100 cd m^{-2}.

In 2009, Law et al. reported triazine-modified Eu^{3+} complex **95** for single-component white EL [97]. The neutral ligand was designed with a combination of triazine and pyrazole groups, while a diethylamine moiety was introduced at the *para*-position of triazine ring to enhance the emission of ligand. This triazole-pyrazole ligand endowed **95** with LUMO of −2.9 eV, beneficial for enhanced electron injection and transport. A typical four-layer device design based on ITO/NPB/CBP:**95**/BCP/Alq_3/LiF/Al showed a white emission with CIE coordinates of (0.34, 0.35) at 16 V and a maximum luminance of ~350 cd m^{-2}.

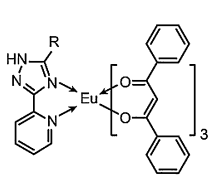

86: R = H
87: R = Ph

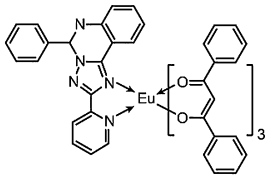

88

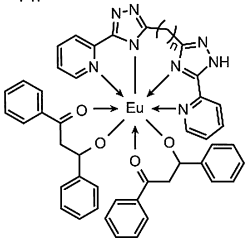

89: n = 1
90: n = 2
91: n = 3

Nitrogen-bearing heterocyclic ligands are among the most sought after system for developing EL Eu^{3+} complexes, with the benefits of efficient LMET, good electron affinity, and robust coordination modes. The extensive investigations reported thus far have demonstrated the significant impact of neutral ligands on EL performance of the resulting Eu^{3+} complexes. However, there are intrinsic constraints limiting sophisticated structure modification. For example, the nitrogen lone pair of the heterocycle used for coordination is sensitive to electron-pushing/withdrawing effects of the functional group. Therefore, functionality should be carefully designed without the concern of losing coordinability. It is also imperative to develop other types of neutral ligands with flexible structures and tunable optoelectronic properties.

3.2.2. *Aryl phosphine oxide-based ligands*

Phosphine oxide (PO) compounds have appeared as promising ligand candidates for preparing EL lanthanide complexes because of the following features: (i) high affinity ligand binding to lanthanide ions; (ii) the inertness of metal-PO bond formation to structural functionalization due to $\sigma_{C\text{-}P}$-blocked electronic communication between the aryl group and oxygen atom; (iii) feasible chemical modification with bulky substituents.

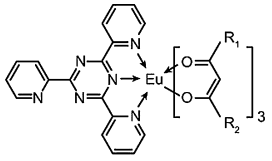

92: R_1 = Ph, R_2 = CF_3 $Eu(BTA)_3TPTZ$
93: R_1 = Th, R_2 = CF_3 $Eu(TTA)_3TPTZ$
94: R_1 = R_2 = CF_3 $Eu(HFAC)_3TPTZ$

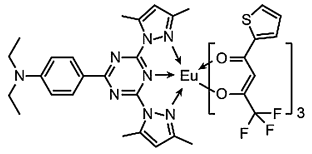

95

In 2000, Hu et al. first constructed EL Eu^{3+} complex **96** with triphenylphosphine oxide (TPPO) and DBM as the neutral and anionic ligand, respectively [98]. The HOMO and LUMO values of this complex were estimated to be −6.4 and −3.6 eV, indicating its electron-transport and hole-blocking abilities. A four-layer device consisting of ITO/TPD/[BCP/**96**]/BCP/Alq_3/LiF/Al achieved a luminance of 380 cd m^{-2} and a maximum CE of ~3 cd A^{-1}. The

effect of the PO ligand on electron injection and transport in EMLs was further demonstrated using complexes **97**–**99**, in which TPPO was used as the neutral ligand while 2-acyl-1,3-indandionate derivatives served as the anionic ligand. These complexes had similar HOMO and LUMO energy levels around −5.6 and −2.6 eV, respectively, effective for hole and electron injection. Among these complexes, **99** showed the best performance with a maximum luminance of 220 cd m^{-2} and a peak CE of 0.1 cd A^{-1} for a simple bilayer device structure (ITO/TPD/**99**/Al) [99].

In order to avoid the problems associated with inadequate coordinating ability of monodentate TPPO ligand, a bidentate PO ligand, bis(2-(diphenylphosphino)phenyl)ether oxide (DPEPO), has been developed by Xu et al. for the generation of EL Eu^{3+} complexes [100]. The chelate structure of DPEPO is formed by linking two TPPO moieties through an ether bridge which provides an added coordination site. As a result, its complex **100** showed T_d of 317 °C, T_m of 167 °C, and T_g of 93 °C. The enhanced thermal and morphological stability is dramatically enhanced as compared with that of $Eu(TTA)_3(TPPO)_2$. A typical four-layer device of ITO/NPB/CBP:**100**/BCP/Alq_3/LiF/Al showed bright and stable pure red emissions from Eu^{3+} on voltage increasing. An impressive maximum luminance of 632 cd m^{-2} was achieved along with maximum efficiencies of 4.58 cd A^{-1}, 2.05 lm W^{-1} and 2.89%.

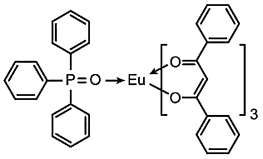

96: $Eu(DBM)_3TPPO$

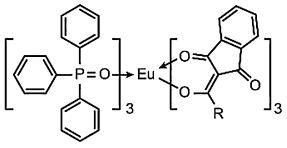

97: R = CH_3 $Eu(AIND)_3(TPPO)_2$

98: R = $Eu(ISOAIND)_3(TPPO)_2$

99: R = $Eu(BIND)_3(TPPO)_2$

Reddy and co-workers also reported devices with red EL based on DPEPO-Eu^{3+} complex **101** [101]. This complex exhibited a PLQE of 28% in thin film form. To enhance the rigidity and reduce structural relaxation-induced energy loss, the same group further employed a xanthene-based PO ligand, DDXPO, for the construction of complex **102** with an improved solid-state PLQE of 48% [102]. Similarly, complex **103** with DDXPO as the neutral ligand exhibited a high PLQE of 47% in chloroform solution, which were further increased to around 80% by doping this complex in PMMA film.

A spiro-fluorene-xanthane-based PO ligand SFXPO was selected to construct Eu^{3+} complexes **104**–**106** for OLED applications [103]. With the spiro structure, SFXPO has extended π-conjugation for electroactivity, well-controlled excitation energy for LMET, and strong site-isolation effects on the magnitude. As a result, SFXPO-based complexes **104**–**106** exhibited intense pure red emissions with improved PLQEs of 55, 62 and 60%, respectively. When blended with CBP and PBD, **104** and **106** showed a further enhancement in the PLQE (~80%), attesting to efficient energy transfer from the CBP:PBD host matrix to the complex. Spin-coated devices fabricated with a structure of ITO/PEDOT:PSS/PVK/CBP:PBD:Eu^{3+} complex/TPBI/LiF/Al showed saturated red emissions with CIE coordinates of (0.65, 0.32) for **104** and (0.66, 0.33) for **106**. The devices based on complex **104** achieved efficiencies of 3.2 cd A^{-1}, 0.6 lm W^{-1} and 2.4% at 100 cd m^{-2}, while complex **106** endowed its devices with higher efficiencies of 5.1 cd A^{-1}, 1.0 lm W^{-1} and 3.7% at 100 cd m^{-2}.

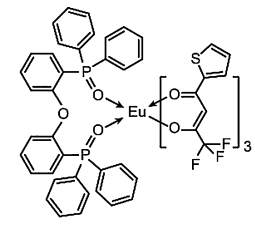

100: $Eu(TTA)_3DPEPO$

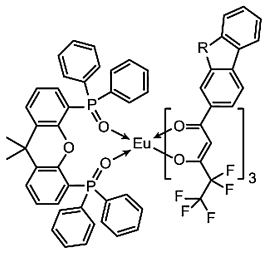

102: R = CH_2 $Eu(pffpd)_3DDXPO$

103: R = NH $Eu(CPFHP)_3DDXPO$

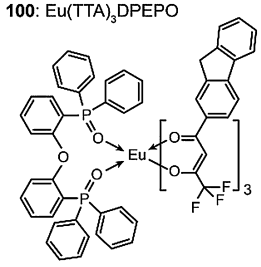

101: $Eu(pffpd)_3DPEPO$

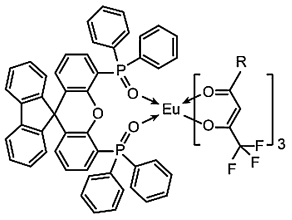

104: R = Th $Eu(TTA)_3SFXPO$

105: R = CF_3 $Eu(HFAC)_3SFXPO$

106: R = Naphthyl $Eu(NTA)_3SFXPO$

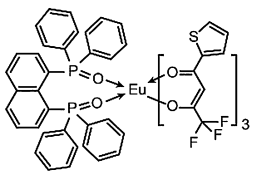

107: $Eu(TTA)_3NAPO$

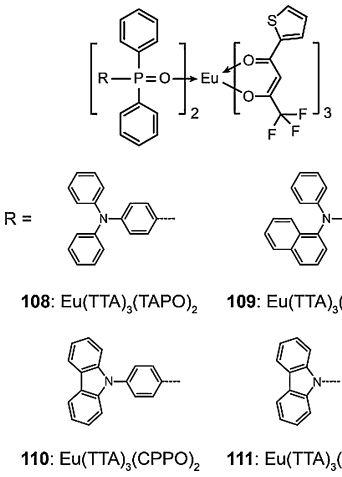

108: $Eu(TTA)_3(TAPO)_2$ **109**: $Eu(TTA)_3(TNADAPO)_2$

110: $Eu(TTA)_3(CPPO)_2$ **111**: $Eu(TTA)_3(CPO)_2$

Xu et al. introduced a naphthyl group into the PO unit of NAPO to improve the rigidity and electroactivity of the ligand [104,105]. NAPO-based complex **107** has T_d of 49 °C, T_m of 271 °C and T_g of 149 °C. These values are considerably higher than those obtained for **100** under identical experimental conditions. Only Eu^{3+}-dominant emissions were observed from **106** in both solution and film. DFT simulation indicated that the substitution of naphthyl in NAPO strongly enhanced its carrier injection ability, leading to higher HOMO and lower LUMO levels than those of TPPO. With a four-layer device configuration (ITO/NPB/CBP:**107**/BCP/Alq_3/LiF/Al), a maximum luminance of 601 cd m^{-2} was achieved together with maximum efficiencies of 2.99 cd A^{-1}, 1.44 lm W^{-1} and 1.89%. The authors argued that the unbalanced charge flux in EML might be the underlying cause for the remarkably high efficiency roll-off.

In 2007, Huang and co-workers reported on the bonding of electron-donating arylamine groups with diphenphosphine oxide (DPPO) to form donor-π-acceptor type (D–π–A) monodentate PO ligands TAPO, NADAPO and CPPO [106,107]. These D–π–A

structures can effectively reduce the S_1 value of TPPO from 4.5 to 3.5 eV, facilitating singlet energy transfer to the S_1 state of TTA (3.1 eV). Concurrently, the T_1 value of these PO ligands reached to 2.9 eV to afford efficient positive triplet energy transfer to the T_1 state of TTA (2.35 eV). As a result, Eu^{3+} complexes **108**–**110** showed high emission efficiencies of 36–40%. The single-layer devices of **108**–**110** (ITO/Eu^{3+} complex/Mg:Ag) gave rise to luminances of 35, 59 and 21 cd m^{-2}, respectively. The EL performance was further improved by employing a four-layer nondoped configuration (ITO/NPB/Eu^{3+} complex/BCP/Alq_3/Mg:Ag). As such, complex **109** displayed excellent performance with a maximum luminance of 1158 cd m^{-2} and maximum efficiencies of 5.88 cd A^{-1}, 3.69 lm W^{-1} and 3.71. Complex **108** showed the highest EL efficiency stability that the maximum efficiencies of its four-layer devices were 5.07 cd A^{-1}, 3.62 lm W^{-1} and 3.2%, which remained as 2.08 cd A^{-1}, 0.63 lm W^{-1} and 1.31% at 100 cd m^{-2}.

Although it was believed that $\sigma_{C\text{-}P}$ bond can effectively block the influence of aryl groups on coordinating ability of P═O moieties, polarizable groups can induce a variation of the potential resonance between P═O and P^+—O^- by changing electron cloud distribution. To validate this hypothesis, Xu et al. designed a D–A type PO ligand CPO and prepared complex **111** for comparison with its D–π–A analog CPPO and the corresponding complex **110** [108]. Both CPO and CPPO ligands showed bipolar structures and comparable FMO energy levels, with direct charge-density contribution to the HOMOs and LUMOs from carbazole and DPPO groups, respectively. However, upon coordination of Eu^{3+}, the HOMO of **111** was 0.2 eV lower than that of **110**, while the LUMO of **111** was 0.4 eV higher than **110**. The authors argued that the formation of coordination bonds in complex **110** would render the localization of negative charges on the O atom of the P═O bond, inducing the shift of electrons from electron-rich carbazole to electron-insufficient DPPO. The direct linkage of carbazole and DPPO in CPO would exacerbate this effect and lead to modest electrical performance of **111**. Indeed, the **111**-based four-layer device (ITO/NPB/**111**/BCP/Alq_3/Mg:Ag) showed a maximum luminance of 399 cd m^{-2} and the maximum efficiencies of 2.66 cd A^{-1}, 0.99 lm W^{-1} and 1.68%, which were estimated to be only 75% of the efficiencies obtained by **110**-based devices. This study clearly demonstrates the superiority of D–π–A ligands in adapting to high coordination uncertainty relative to D–A ligands.

The distinct ligand emission as shown in the PL spectra of **108**–**111** in solution indicates an inefficient LMET partly due to structural relaxation of the excited states and solvent effects. With the advantages of PO ligands factored in, especially their ability to form compact coordination configuration, Xu et al. prepared bidentate PO ligands by utilizing hole transport groups to connect two DPPO moieties [109]. PL spectra of DPPO-based complexes **112**–**114** in dichloromethane solution only consisted of neat Eu^{3+}-originated emissions with a PLQE of ~35% and lifetime of ~400 μs. With the help of bidentate PO ligands, high T_d values of more than 310 °C were obtained for **112**–**114**. The bidentate PO ligands endowed their complexes with strong electron injecting ability, as evident by their LUMO values in the range from −2.8 to −3.3 eV. Their HOMO energy levels of **112**–**114** (−5.1 to −5.6 eV) were consistent with the electron-donating ability of the hole transport groups in the PO ligands. With a four-layer device structure of ITO/NPB/CBP:Eu^{3+} complex/BCP/Alq_3/Mg:Ag, **114**-based devices showed a maximum luminance of 1176 cd m^{-2} and maximum efficiencies of 5.1 cd A^{-1}, 2.3 lm W^{-1} and 3.2%. Another bidentate PO ligand EFDPO with a fluorene group was also used to construct Eu^{3+} coordination polymer **115** for EL application. An improved thermal and morphological stability (T_d = 325 °C, T_m = 249 °C and T_g = 112 °C) was observed for this metal-polymer complex. The four-layer devices made of **115** achieved a luminance of 603 cd m^{-2} and maximum efficiencies of 3.5 cd A^{-1}, 1.2 lm W^{-1} and 2.2%.

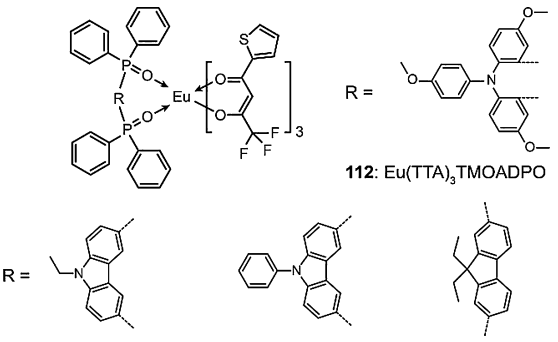

Recently, Xu and co-workers developed an effective post-functionalization strategy to construct PO-Eu^{3+} chelates **116**–**135** with self-hosted feature, ambipolar characteristics, and enhanced solubility [110]. By introducing carrier transport groups at the 4- and 4′-positions of DPEPO, the ratio of organic components in these complexes can be increased to enhance their solubility in common organic solvents, thereby facilitating device fabrication by solution-processable techniques. Notably, a high PLQE of 86% was achieved for **116** and **120**. DFT simulation suggested the involvement of carrier transport groups in the corresponding occupied MOs, indicating the effect of the functionalization on carrier transporting ability of the complexes. This effect was further examined by CV analysis, confirming that the HOMO energy levels of the complexes are in accord with the electron-donating ability of the functional groups in the PO ligands, while their LUMO energy levels are mainly determined by their β-diketonate ligands. Taken together, these studies provide evidence for the existence of self-hosts in metal complexes [111–113]. With a simple single-layer spin-coated device structure of ITO/PEDOT:PSS/PVK:PBD:Eu^{3+} complex/Ca/Al, pure red emissions were demonstrated with remarkably reduced driving voltages, such as a low turn-on voltage of 6 V. Compared with their analogs, **120** and **133** endowed their devices with the biggest luminance of 71 and 95 cd m^{-2}, accompanied with the highest efficiencies with the maxima of 0.09 cd A^{-1} and 0.04%. Accordingly, small-molecular Eu^{3+} complexes can be competent as emitters in spin-coated devices with rational function integration.

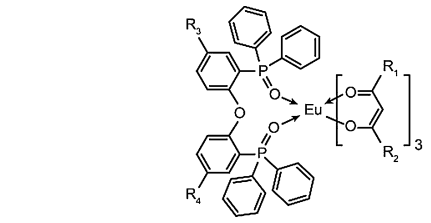

R_1 = CF_3, R_2 = Th		R_1 = R_2 = Ph
R_3 =H, R_4 = Cz	**116**: $Eu(TTA)_3DPEPOCz$	**126**: $Eu(DBM)_3DPEPOCz$
R_3 = R_4 = Cz	**117**: $Eu(TTA)_3DPEPOCz2$	**127**: $Eu(DBM)_3DPEPOCz2$
R_3 =H, R_4 = PhCz	**118**: $Eu(TTA)_3DPEPOPhCz$	**128**: $Eu(DBM)_3DPEPOPhCz$
R_3 = R_4 = PhCz	**119**: $Eu(TTA)_3DPEPOPhCz2$	**129**: $Eu(DBM)_3DPEPOPhCz2$
R_3 =H, R_4 = TPA	**120**: $Eu(TTA)_3DPEPOTPA$	**130**: $Eu(DBM)_3DPEPOTPA$
R_3 = R_4 = TPA	**121**: $Eu(TTA)_3DPEPOTPA2$	**131**: $Eu(DBM)_3DPEPOTPA2$
R_3 =H, R_4 = DPNA	**122**: $Eu(TTA)_3DPEPODPNA$	**132**: $Eu(DBM_3DPEPODPNA$
R_3 = R_4 = DPNA	**123**: $Eu(TTA)_3DPEPODPNA2$	**133**: $Eu(DBM)_3DPEPODPNA2$
R_3 =H, R_4 = DEF	**124**: $Eu(TTA)_3DPEPODEF$	**134**: $Eu(DBM)_3DPEPODEF$
R_3 = R_4 = DEF	**125**: $Eu(TTA)_3DPEPODEF2$	**135**: $Eu(DBM)_3DPEPODEF2$

PO compounds have exhibited their great potential as functional ligands for preparing EL Eu^{3+} complexes with the benefits of strong coordination and easy of multi-function integration. Nevertheless, the investigation of this kind of neutral ligands is still at an early stage. Their superiorities are not thoroughly unfolded. The EL performance of their Eu^{3+} complexes was far from what was expected. A systematic study of PO ligands involving in optical and electrical processes is imperative to guide the subsequent development of highly efficient EL PO Eu^{3+} complexes.

3.3. Polymeric Eu^{3+} complexes for electroluminescence

Polymeric light-emitting diodes (PLED) are believed to be superior in large-scale and low-cost applications in display and lighting, owing to the unique solution processability of polymeric materials, such as spin-coating, screen printing and inkjet printing technologies [114]. However, as mixtures of homologues with different chain lengths and conjugations, emission bands of polymeric emitters are largely broadened, resulting in their color purity lower than those of their small molecular counterparts. Obviously, incorporation of lanthanide ions in these polymers can improve the emission color purity with the prerequisite of efficient positive energy transfer from polymeric skeletons to lanthanide ions [115]. In this sense, polymeric components in lanthanide metallopolymers are actually macromolecular ligands with three functions: (i) serving as matrices to disperse emissive lanthanide-involved cores for suppressed luminescence quenching; (ii) Improving electroactivity of the materials; and (iii) capturing excitons and then transferring energy to the complex cores for lanthanide emissions. Commonly, two approaches were employed to prepare Eu^{3+}-containing metallopolymers as (i) Pre-coordination method. Complexes with polymerizable ligands were first prepared and then used as comononor to form final copolymers; (ii) Post-coordination method. Polymeric skeletons with coordination sites were first prepared and then chelated with Eu^{3+} complex units. For the pre-method, the stability of complex monomer during polymerization should be considered, while for the post-method, because of the wrapping of the coordination sites by polymeric chains, the control of Eu^{3+} concentration remains a challenge.

Polyacrylate is known as one of the best optical materials with light transmittance beyond 80%, making this structure competent as an inert matrix for dispersing Eu^{3+}-involved emissive cores. Yan et al. synthesized a copolymer with a repeat unit of maleic acid (MA) and methyl methacrylate (MMA). The carboxylic group of MA provided the coordination site for Eu^{3+} ion [116]. Using this polymer as the ligand, a Eu^{3+}-containing polymer complex **136** was prepared with $Eu(TTA)_2Phen$ as emissive core. As expected, only the Eu^{3+} segment of the complex contributed to the absorption and emission of the polymer. When excited at 395 nm, complex **136** displayed a PLQE of 24%. Under an electrical field, complex **136**-coated InGaN chips afforded a pure red emission with CIE coordinates of (0.62, 0.32) and a PE of 3.65 lm W^{-1}. Another typical ternary Eu^{3+} complex segment $Eu(DBM)_2Phen$ was incorporated, along with an epoxyethyl group, into the PMMA skeleton as side groups [117]. The epoxy group provided photocrosslinkability for photolithographic device fabrication. The resulting polymer **137** showed pure red emissions from Eu^{3+}. After crosslinking, its T_d value was improved to 295 °C with an increase of 48 °C. The root-mean-square (RMS) surface roughness of the crosslinked thin film was as low as 0.295 nm. Xu et al. introduced $Eu(TTA)_2$ into the PMMA matrix to form complex **138** using the anchoring site of hydroxyquinoline [118]. An improved PLQE of 45% for **138** was achieved at an Eu^{3+} concentration of 5% with an elongated lifetime of 630 μs, implying the site isolation effect of PMMA matrix. When further increasing Eu^{3+} content, remarkable emission quenching was observed. Obviously, uniform dispersion of Eu^{3+} monomer in PMMA matrix was beneficial to suppress the interactions between emissive cores and thereby reduce quenching effect. Instead of rigid 1,10-phenanthroline, Yan et al. used trioctylphosphine oxide (TOPO) with long aliphatic chains as the neutral ligand to improve the compatibility of Eu^{3+}-containing monomer with MMA [119]. The average molecular weight of polymer **139** was 20 times higher than that of its analog **136**. Complex **139** inherited the high thermal and morphological stability from its skeleton with T_d and T_g of 340 and 90 °C, respectively. On 395 nm excitation, only Eu^{3+} emission centering at about 617 nm was observed with a PLQE of 18% and a lifetime of 373 μs.

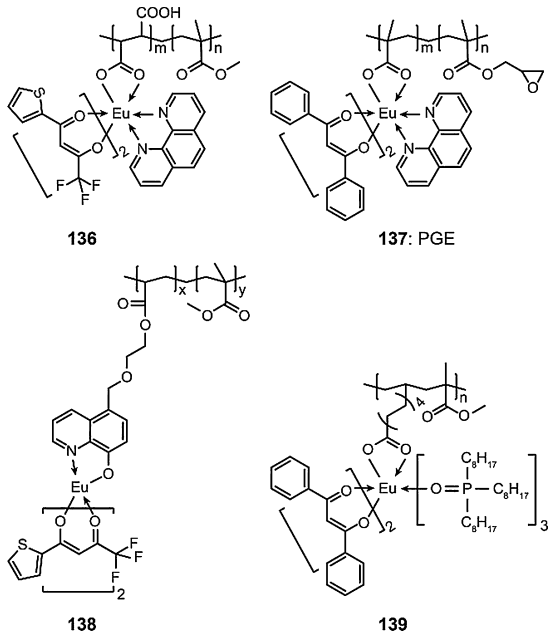

In spite of excellent optical properties offered by PMMA materials, their insulativity restrained charge injection and transport. PVK is a common polymeric host utilized in Eu^{3+} complex-based devices with attributes of high excited energy levels and good hole injecting/transporting ability. Yang et al. reported the first example of Eu^{3+}-containing PVK polymer **140** with an intense red emission centered at 614 nm [120]. A simple single-layer device of ITO/**140**/Al can be turned on at a driving voltage of 17 V, with a maximum luminance of 16 cd m^{-2} and a PE of 0.25 lm W^{-1}. Kang and co-workers used 4-vinylbenzoic acid as a polymerizable ligand to construct Eu^{3+}-complexing monomers [121]. After copolymerization with vinylcarbazole, polymer **141** with high molecular weights over 10,000 could be synthesized. Transmission electron microscope (TEM) imaging indicated the remarkably improved film uniformity of **141** as compared with the blend of PVK and Eu^{3+}-complexing monomers. The single-layer devices of **141** (ITO/**141**/Ca:Ag) showed outstanding performance, with a turn-on voltage of 8 V, a maximum luminance of 126 cd m^{-2}, and a maximum CE of 0.56 cd A^{-1}.

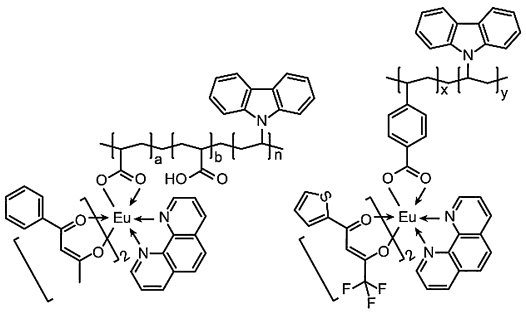

140 141

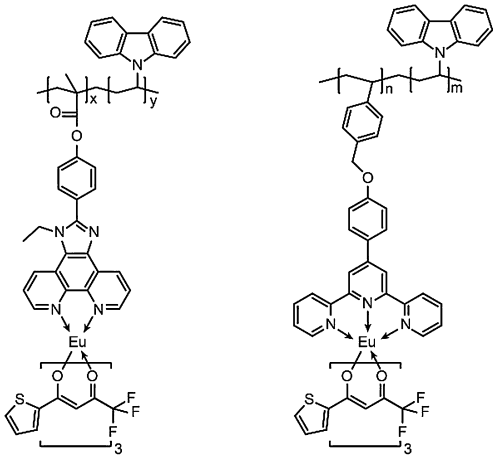

142 143

In 2009, Zhang's group reported the synthesis of polymeric Eu^{3+} complex **142** by incorporating EPIP as the neutral anchoring site into a PVK-MMA-based skeleton [122]. The number-average molecular weight (M_n) of **142** was relatively small (<5000). For good measure, to have strong durable mechanical properties, the polymer typically has to have a molecular weight of much larger than 10,000 for structural applications. The reason for the low molecular weight of **142** lies in conformational effects arising from the steric bulkiness of the Eu^{3+} monomer. Nevertheless, **142** possessed good thermal and morphological stability with T_d and T_g of 347 and 200 °C, respectively. Distinct Eu^{3+} emission was observed in the PL spectra of **142** in chloroform solution or in solid state. The trilayer device fabricated with the structure of ITO/PEDOT:PSS/**142**/BCP/Alq_3/LiF/Al gave rise to pure red emission, with a maximum luminance of 42 cd m^{-2} and peak efficiencies of 0.27 cd A^{-1} and 0.035 lm W^{-1}. To enhance the structural stability and emissive performance of the monomer complex, a polymerizable tridentate ligand with terpyridine as the anchoring site was incorporated through a long and flexible linker to reduce the level of steric hindrance during the polymerization [123]. After copolymerization with vinylcarbazole, polymer **143** with a molecular weight of more than 10,000 was prepared. Although the emission from the PVK segment was strong in THF solution due to the solvent-suppressed interchain energy transfer, only pure red emission at 614 nm from Eu^{3+} was observed in solid states with a long lifetime over 600 μs and a PLQE about 38%. As the main component, the PVK segment determined the redox behavior of the copolymer, resulting in the HOMO and LUMO values around −5.7 and −2.2 eV, respectively. With a bilayer device structure of ITO/PEDOT:PSS/PVK/**143**:OXD-7/Ba/Al, a maximum luminance of 68 cd m^{-2} and maximum efficiencies of 0.18 cd A^{-1}, 0.031 lm W^{-1} and 0.37% were obtained.

Considering the prerequisite of structural stability of complex monomer during polymerization, the strong coordination ability and flexible coordination mode of PO ligands made them attractive as polymerizable neutral ligands for Eu^{3+} metallopolymers. In 2011, Xu et al. first utilized **113** as an emissive core and pendent group to form polymer **144** [124]. As expected, the M_n of **144** increased to more than 9500 with an Eu^{3+} content of 0.8%. The copolymer showed good thermal and morphological stability, with T_d and T_g values of 340 and 200 °C, respectively. The PL spectrum of **144** only consists of Eu^{3+} emission centering at 615 nm with a PLQE of 60%. The authors attributed the high quantum efficiency to the positive singlet and triplet intrachain energy transfer from PVK segment and PO ligand with high S_1 and T_1 values (~3.5 and ~2.9 eV, respectively). The single-layer spin-coated devices were fabricated with the configuration of ITO/PEDOT:PSS/**144**:PBD/Ba/Al, enabling pure red emissions with a maximum luminance of 36 cd m^{-2}. Taking account of electron-withdrawing effect of P=O moieties, hole injecting ability of carbazole group in PO ligand was remarkably weaker than that of PVK segment, while the situation for electron injecting ability was exactly the opposite. In this case, hole and electron traps would be formed on PVK and Eu^{3+}-complexed segments, respectively, to generate charge transfer type excitons, which were easily decomposed and deactivated through nonradiative processes. This was the main reason for the low luminance of **144**-based devices.

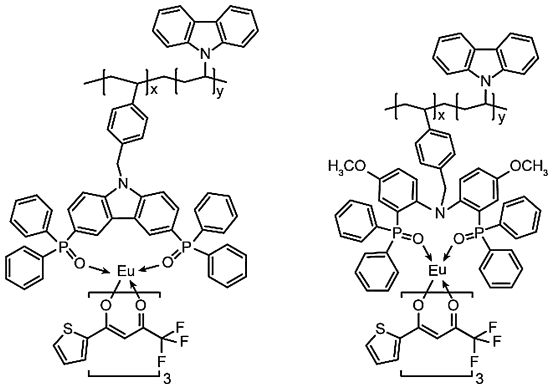

144 145

With this consideration in mind, the same authors employed methoxyl-substituted diphenylamine with strong electron-donating ability in a polymerizable PO ligand to form complex **145** [125]. DFT simulation on a model segment containing two carbazole groups and one PO ligand indicated that both the HOMO and LUMO of this segment were localized on the PO ligand to form hole and electron traps with depths of 0.16 and 0.13 eV, respectively. This structural arrangement promotes the formation of localized Frenkel excitons in favor of high radiative probability. Relative to complex **144**, complex **145** displayed better thermal and morphological stability with higher T_d (430 °C) and T_g (220 °C) values, largely attributable to the flexible structure of diphenylamine group. The devices utilizing complex **145** gave rise to an impressive EL performance, including a maximum brightness of 149 cd m^{-2} and the maximum efficiencies of 0.41 cd A^{-1}, 0.09 lm W^{-1} and 0.43% at a luminance of 72 cd m^{-2}.

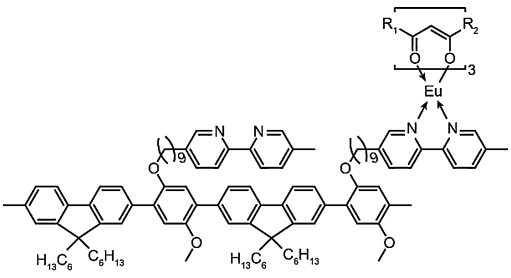

146: $R_1 = R_2 = Ph$
147: $R_1 = Th$, $R_2 = CF_3$
148: $R_1 = Naphthyl$, $R_2 = CF_3$

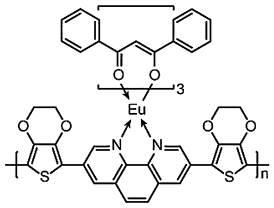

149

Conjugated backbones with defined optoelectronic properties are superior to aliphatic skeletons in many aspects, such as sensitizability and carrier injection and transport ability. For instance, Pei et al. designed a macromolecular ligand bearing a main polyfluorene (PF) chain and pendent chelating bpy for Eu^{3+} [126]. With $Eu(DBM)_3$, $Eu(TTA)_3$ and $Eu(NTA)_3$ as emissive cores, the authors constructed polymer complexes **146**–**148**, respectively. Notably, complex **146** gave rise to a strong emission of Eu^{3+} at 612 nm, accompanied with a weak PF emission at 420 nm. The strong emission of Eu^{3+} can be ascribed to facile energy transfer from the polymeric skeleton to Eu^{3+} as a result of good spectral overlap between the absorption of pendent $Eu(DBM)_3$ unit and the emission of PF backbone. The bilayer device of ITO/PVK/**146**/Ba/Al afforded pure red emissions from Eu^{3+} with a maximum luminance of 11 cd m^{-2} and a peak EQE of 0.07%.

The PF emission observed in PL spectra of polymer complexes **146**–**148** indicates incomplete energy transfer between the molecular backbones to pendent chelating groups. Therefore, it is rational to develop metallopolymers with Eu^{3+} chelates embedded in skeletons for improved efficiency of intra-chain energy transfer. As an excellent demonstration, Holliday and co-workers constructed a novel polymer complex **149** by electropolymerization of thiophenyl-modified 1,10-phenanthroline [127]. The film made of complex **149** showed good electroconductibility and purely red emission. In a parallel development, Huang and coworkers synthesized an interesting metallopolymer complex **150** by inserting a bpy unit into the PF backbone to chelate $Eu(TTA)_3$ as emissive cores [128]. The pendent oxetane group in complex **150** provides further photo-crosslinkability. In thin film form, complex **150** showed predominant Eu^{3+} emissions with the main peak centered at 612 nm. However, upon crosslinking the complex exhibited enhanced PF emissions arising from suppressed interchain energy transfer in three-dimensional crosslinked structures. Similarly, the fluorene unit in complex **151** was modified with a bpy unit at its 4-position through a C=C linker, allowing high levels of Eu^{3+} (up to 80%) to be used [129]. Nevertheless, the twist configuration of the polymer suppressed the intrachain energy transfer and resulted in weak Eu^{3+} emissions in the PL and EL spectra.

Chandrasekar and co-workers developed a series of fully conjugated Eu^{3+}-containing polymers **152**–**155** with tridentate coordination sites for Eu^{3+} chelates [130,131]. The polymer backbones emitted greenish blue light in thin film form with two peaks around 450 and 550 nm, attributable to single chain and aggregation state emissions, respectively. When immersed in $Eu(TTA)_3$ solutions, the pure white emission with CIE coordinates close to (0.33, 0.33) from the coated films can be achieved by controlling the complex concentration.

Most recently, Xu et al. further demonstrated the first electroluminescent Wolf-III type Eu^{3+} complex **156** with a bidentate FDPO ligand for bridging $Eu(DBM)_3$ repeating units. [132]. The stability issue of its one-dimensional-chain structure during the device fabrication by spin coating was successfully solved by virtue of strong binding ability of the FDPO ligand. Complex **156** showed a high solid-state PLQE of more than 80% and a suitable LUMO energy level of −2.6 eV for effective electron injection. Significantly, its Wolf-III type configuration supported peculiar intra-chain carrier transport and rendered a high electron mobility of 10^{-6} cm^2 V^{-1} s^{-1}. The double-layer spin-coated devices made of **156** realized unique single-polymer white emission, accompanied with a reduced drive voltage of 10.2 V at 100 cd m^{-2} and high luminance and efficiency up to 215 cd m^{-2} and 0.71 cd A^{-1}, respectively. The authors attributed the improved optoelectronic performance of **156** to the function of FDPO as an effective bridge in both intra-chain energy and charge transfer processes.

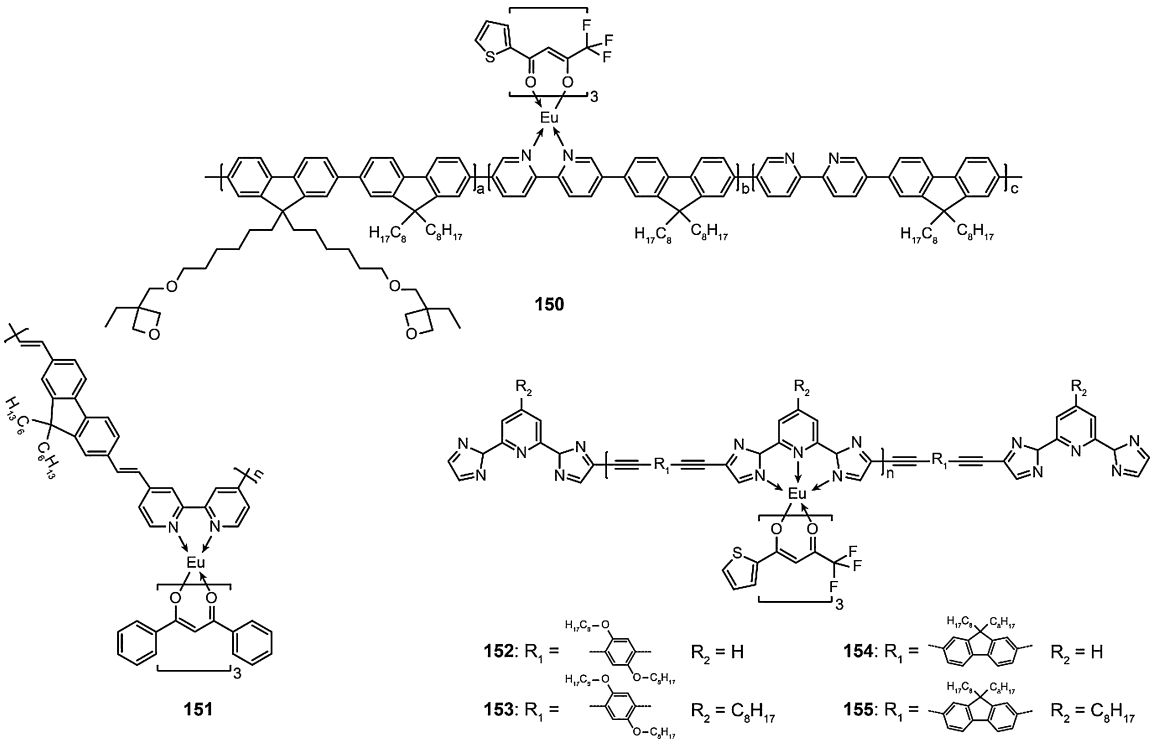

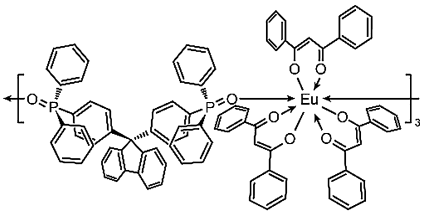

156: Eu-FDPO

Despite improved optoelectronic performance of Eu^{3+} metallopolymers, their EL performance is still considerably worse than that of their small-molecular congeners. The key problems may lie in the incompatibility of polymeric sketelons with Eu^{3+} during energy transfer and charge transfer processes. A future task would be the specific design of functional comonomers with suitable excited state characteristics and FMO levels.

4. Conclusions

High performance EL Eu^{3+} complexes will continue to be developed at a fast pace not only because they provide high color purity for high-resolution displays but enable potential applications in optical communication and lasing. Despite the concerns over low their luminance and EQE, the monochromic red emission and wide bandgap of Eu^{3+} complexes make them irreplaceable among red emitters. Indeed, the emission peak area of the Eu^{3+} complex is typically a tenth of what is measured for purely organic dyes. For good measure, top ranked EL Eu^{3+} complexes have a luminance of $\sim$2000 cd m^{-2} and an EQE of $\sim$4%, which is about a 10-fold increase as opposed to other state-of-art red phosphors. Nevertheless, the EL efficiencies of these materials are much lower than achievable for their PL efficiencies, largely owing to different excitation processes and the quenching effects. Furthermore, although rarely discussed explicitly, many researchers hold the view that the stability of Eu^{3+} complexes under an electric field is another major issue limiting their EL performance. This issue can be addressed by increasing the binding strength between ligands and Eu^{3+} ions or through the use of ligands possessing reversible or quasi-reversible redox behavior. Looking ahead, further improvement will likely focus on enhancing the electroactivity of the complexes, optimizing intramolecular energy transfer, and increasing molecular stability and film formability.

Acknowledgements

X.L. acknowledges the National Research Foundation and the Economic Development Board (Singapore-Peking-Oxford Research Enterprise, COY-15-EWI-RCFSA/N197-1), the Ministry of Education (MOE2010-T2-1-083), and the Agency for Science, Technology and Research (A*STAR) for providing support during the time this Review was written. H.X. acknowledges financial support from National Natural Science Fund of China (NSFC, 61176020 and 51373050), New Century Excellent Talents Supporting Program of MOE (NCET-12-0706), Key Project of MOE (212039) and the Fok Ying-Tong Education Foundation for Young Teachers in the Higher Education Institutions of China (141012).

References

[1] H. Xu, R. Chen, Q. Sun, W. Lai, Q. Su, W. Huang, X. Liu, Chem. Soc. Rev. 43 (2014) 3259–3302.
[2] Y. Wu, W. Zhu, Chem. Soc. Rev. 42 (2013) 2039–2058.
[3] S. Gong, C. Yang, J. Qin, Chem. Soc. Rev. 41 (2012) 4797–4807.
[4] C.-L. Ho, W.-Y. Wong, Coord. Chem. Rev. 257 (2013) 1614–1649.
[5] G.M. Farinola, R. Ragni, Chem. Soc. Rev. 40 (2011) 33467–33482.
[6] Y. Chi, P.-T. Chou, Chem. Soc. Rev. 39 (2010) 638–655.
[7] F. Wang, X. Liu, Chem. Soc. Rev. 38 (2009) 976–989.
[8] K. Binnemans, Chem. Rev. 109 (2009) 4283–4374.
[9] F. Wang, R. Deng, J. Wang, Q. Wang, Y. Han, H. Zhu, X. Chen, X. Liu, Nat. Mater. 10 (2011) 968–973.
[10] Q. Su, S. Han, X. Xie, H. Zhu, H. Chen, C.K. Chen, R.S. Liu, X. Chen, F. Wang, X. Liu, J. Am. Chem. Soc. 134 (2012) 20849–20857.
[11] Q.P. Li, B. Yan, Photochem. Photobiol. Sci. 12 (2013) 1628–1635.
[12] J.-C.G. Bunzli, C. Piguet, Chem. Soc. Rev. 34 (2005) 1048–1077.
[13] Y. Ma, Y. Wang, Coord. Chem. Rev. 254 (2010) 972–990.
[14] L. Armelao, S. Quici, F. Barigelletti, G. Accorsi, G. Bottaro, M. Cavazzini, E. Tondello, Coord. Chem. Rev. 254 (2010) 487–505.

[15] F.-F. Chen, Z.-Q. Chen, Z.-Q. Bian, C.-H. Huang, Coord. Chem. Rev. 254 (2010) 991–1010.
[16] M.A. Baldo, D.F. O'Brien, Y. You, A. Shoustikov, S. Sibley, M.E. Thompson, S.R. Forrest, Nature 395 (1998) 151–154.
[17] W. Huang, B. Mi, Z. Gao, Organic Electronics, 1st ed., Science Press, Beijing, 2011.
[18] S.I. Weissman, J. Chem. Phys. 10 (1942) 214–217.
[19] D.L. Dexter, J. Chem. Phys. 21 (1953) 836–850.
[20] G.A. Crosby, R.E. Whan, R.M. Alire, J. Chem. Phys. 34 (1961) 743–748.
[21] M.L. Bhaumik, M.A. El-Sayed, J. Phys. Chem. 69 (1965) 275–280.
[22] M. Latva, H. Takalo, V.-M. Mukkala, C. Matachescu, J.C. Rodríguez-Ubis, J. Kankare, J. Lumin. 75 (1997) 149–169.
[23] H. Xin, M. Shi, X.C. Gao, Y.Y. Huang, Z.L. Gong, D.B. Nie, H. Cao, Z.Q. Bian, F.Y. Li, C.H. Huang, J. Phys. Chem. B 108 (2004) 10796–10800.
[24] H. Xu, W. Huang, J. Photochem. Photobiol. A 217 (2011) 213–218.
[25] K. Binnemans, Coord. Chem. Rev. (2015), http://dx.doi.org/10.1016/j.ccr.2015.02.015.
[26] J. Kido, K. Nagai, Y. Okamoto, T. Skotheim, Chem. Lett. 20 (1991) 1267–1270.
[27] J. Kido, K. Nagai, Y. Okamoto, J. Alloy Compd. 192 (1993) 30–33.
[28] J. Kido, H. Hayase, K. Hongawa, K. Nagai, K. Okuyama, Appl. Phys. Lett. 65 (1994) 2124–2126.
[29] S. Takeshi, F. Masayuki, F. Takanori, H. Yuji, S. Kenichi, K. Kazuhiko, Jpn. J. Appl. Phys. 34 (1995) 1883–1887.
[30] M.R. Robinson, M.B. O'Regan, G.C. Bazan, Chem. Commun. (2000) 1645–1646.
[31] P. He, H.H. Wang, S.G. Liu, J.X. Shi, G. Wang, M.L. Gong, Inorg. Chem. 48 (2009) 11382–11387.
[32] P. He, H.H. Wang, S.G. Liu, J.X. Shi, M.L. Gong, Appl. Phys. B 99 (2010) 757–762.
[33] S.-G. Liu, R.-K. Pan, X.-P. Zhou, X.-L. Wen, Y.-Z. Chen, S. Wang, X.-B. Shi, Inorg. Chim. Acta 395 (2013) 119–123.
[34] S.-G. Liu, W.-Y. Su, R.-K. Pan, X.-P. Zhou, X.-L. Wen, Y.-Z. Chen, S. Wang, X.-B. Shi, Spectrochim. Acta A 103 (2013) 417–422.
[35] S. Li, G. Zhong, W. Zhu, F. Li, J. Pan, W. Huang, H. Tian, J. Mater. Chem. 15 (2005) 3221–3228.
[36] H. Liang, F. Xie, Spectrochim. Acta A 75 (2010) 1191–1194.
[37] T. Zhang, Z. Xu, L. Qian, D.L. Tao, F. Teng, X. Gao, X.R. Xu, Chem. Phys. Lett. 415 (2005) 30–33.
[38] Y. Zheng, F. Cardinali, N. Armaroli, G. Accorsi, Eur. J. Inorg. Chem. (2008) 2075–2080.
[39] Y. Zheng, Y. Zhou, G. Accorsi, N. Armaroli, J. Rare Earths 26 (2008) 173–177.
[40] L. Zhang, B. Li, L. Zhang, Z. Su, ACS Appl. Mater. Interfaces 1 (2009) 1852–1855.
[41] H. Wang, P. He, H. Yan, J. Shi, M. Gong, Inorg. Chem. Commun. 14 (2011) 1183–1185.
[42] N.-J. Xiang, L.M. Leung, S.-K. So, M.-L. Gong, Spectrochim. Acta A 65 (2006) 907–911.
[43] N. Xiang, Y. Xu, Z. Wang, X. Wang, L.M. Leung, J. Wang, Q. Su, M. Gong, Spectrochim. Acta A 69 (2008) 1150–1153.
[44] N.J. Xiang, L.M. Leung, S.K. So, J. Wang, Q. Su, M.L. Gong, Mater. Lett. 60 (2006) 2909–2913.
[45] R. Tang, W. Zhang, Y. Luo, J. Li, J. Rare Earths 27 (2009) 362–367.
[46] M. Shi, F. Li, T. Yi, D. Zhang, H. Hu, C. Huang, Inorg. Chem. 44 (2005) 8929–8936.
[47] C.W. Tang, S.A. VanSlyke, Appl. Phys. Lett. 51 (1987) 913–915.
[48] G. Zucchi, V. Murugesan, D. Tondelier, D. Aldakov, T. Jeon, F. Yang, P. Thuery, M. Ephritikhine, B. Geffroy, Inorg. Chem. 50 (2011) 4851–4856.
[49] Y. Liu, J. Li, C. Li, J. Song, Y. Zhang, J. Peng, X. Wang, M. Zhu, Y. Cao, W. Zhu, Chem. Phys. Lett. 433 (2007) 331–334.
[50] Y. Liu, Y. Wang, H. Guo, M. Zhu, C. Li, J. Peng, W. Zhu, Y. Cao, J. Phys. Chem. C 115 (2011) 4209–4216.
[51] Y. Liu, Y. Wang, C. Li, Y. Huang, D. Dang, M. Zhu, W. Zhu, Y. Cao, Mater. Chem. Phys. 143 (2014) 1265–1270.
[52] L. Li, Y. Liu, H. Guo, Y. Wang, Y. Cao, A. Liang, H. Tan, H. Qi, M. Zhu, W. Zhu, Tetrahedron 66 (2010) 7411–7417.
[53] Y. Liu, J. Wang, Y. Wang, Z. Zhang, M. Zhu, G. Lei, W. Zhu, Dyes Pigments 95 (2012) 322–329.
[54] Y. Liu, K. Chen, K. Xing, Y. Wang, H. Jiang, X. Deng, M. Zhu, W. Zhu, Tetrahedron 69 (2013) 4679–4686.
[55] P.-P. Sun, J.-P. Duan, J.-J. Lih, C.-H. Cheng, Adv. Funct. Mater. 13 (2003) 683–691.
[56] X.-N. Li, Z.-J. Wu, Z.-J. Si, Z. Liang, X.-J. Liu, H.-J. Zhang, Phys. Chem. Chem. Phys. 11 (2009) 9687–9695.
[57] Y. Liu, Y. Wang, J. He, Q. Mei, K. Chen, J. Cui, C. Li, M. Zhu, J. Peng, W. Zhu, Y. Cao, Org. Electron. 13 (2012) 1038–1043.
[58] X. Liu, G. Xiao, H. Chi, Y. Dong, H. Zhao, P. Lei, Z. Zhang, Z. Hu, S. Wu, Z. Su, W. Li, Mater. Chem. Phys. 123 (2010) 289–292.
[59] J. Sun, G. Hu, Q. She, Z. Zuo, L. Guo, Spectrochim. Acta A 91 (2012) 192–197.
[60] A. Pereira, G. Conte, H. Gallardo, C. Zucco, W.G. Quirino, C. Legnani, M. Cremona, I.H. Bechtold, J. Soc. Inf. Disp. 19 (2011) 793–797.
[61] Z. Bian, D. Gao, M. Guan, H. Xin, F. Li, C. Huang, K. Wang, L. Jin, Sci. China Chem. 47 (2004) 326–334.
[62] Z.-Q. Bian, K.-Z. Wang, L.-P. Jin, Polyhedron 21 (2002) 313–319.
[63] Z. Bian, D. Gao, K. Wang, L. Jin, C. Huang, Thin Solid Films 460 (2004) 237–241.
[64] H. Xin, F.Y. Li, M. Guan, C.H. Huang, M. Sun, K.Z. Wang, Y.A. Zhang, L.P. Jin, J. Appl. Phys. 94 (2003) 4729–4731.
[65] H. Xin, M. Sun, K.Z. Wang, Y.A. Zhang, L.P. Jin, C.H. Huang, Chem. Phys. Lett. 388 (2004) 55–57.
[66] M. Guan, Z.Q. Bian, F.Y. Li, H. Xin, C.H. Huang, N. J. Chem. 27 (2003) 1731–1734.
[67] M. Sun, H. Xin, K.Z. Wang, Y.A. Zhang, L.P. Jin, C.H. Huang, Chem. Commun. (2003) 702–703.
[68] Q. Xue, P. Chen, J. Lu, G. Xie, J. Hou, S. Liu, Y. Zhao, L. Zhang, B. Li, Solid State Electron. 53 (2009) 397–399.
[69] Y. Li, J. Lumin. 132 (2012) 2102–2108.
[70] J. Yuan, J. Li, L.M.L. Leung, S. So, J. Yao, M. Gong, Chem. J. Chin. Univ. 26 (2005) 1787–1790.
[71] H. Tang, H. Tang, Z. Zhang, J. Yuan, C. Cong, K. Zhang, Synth. Met. 159 (2009) 72–77.
[72] G. Santos, F.J. Fonseca, A.M. Andrade, V. Deichmann, L. Akcelrud, S.S. Braga, A.C. Coelho, I.S. Gonçalves, M. Peres, W. Simões, T. Monteiro, L. Pereira, J. Non-Cryst. Solids 354 (2008) 2897–2900.
[73] C.R. De Silva, F. Li, C. Huang, Z. Zheng, Thin Solid Films 517 (2008) 957–962.
[74] Y.-Y. Wang, L.-H. Wang, X.-H. Zhu, J. Ru, W. Huang, J.-F. Fang, D.-G. Ma, Synth. Met. 157 (2007) 165–169.
[75] H. You, J. Fang, J. Gao, D. Ma, J. Lumin. 122 (2007) 687–689.
[76] X.-H. Zhu, L.-H. Wang, J. Ru, W. Huang, J.-F. Fang, D.-G. Ma, J. Mater. Chem. 14 (2004) 2732–2734.
[77] H. You, J. Fang, L. Wang, X. Zhu, W. Huang, D. Ma, Opt. Mater. 29 (2007) 1514–1517.
[78] Z. Liu, F. Wen, W. Li, Thin Solid Films 478 (2005) 265–270.
[79] S. Wang, J. Zhang, Y. Hou, C. Du, Y. Wu, J. Mater. Chem. 21 (2011) 7559–7561.
[80] L. Huang, K.-Z. Wang, C.-H. Huang, F.-Y. Li, Y.-Y. Huang, J. Mater. Chem. 11 (2001) 790–793.
[81] K. Wang, L. Gao, C. Huang, J. Photochem. Photobiol. A 156 (2003) 39–43.
[82] F. Liang, Q. Zhou, Y. Cheng, L. Wang, D. Ma, X. Jing, F. Wang, Chem. Mater. 15 (2003) 1935–1937.
[83] L. Zhang, T. Li, B. Li, B. Lei, S. Yue, W. Li, J. Lumin. 126 (2007) 682–686.
[84] H. Wang, P. He, S. Liu, J. Shi, M. Gong, Appl. Phys. B 97 (2009) 481–487.
[85] H. Wang, P. He, S. Liu, J. Shi, M. Gong, Inorg. Chem. Commun. 13 (2010) 145–148.
[86] L. Chen, B. Wang, L. Zhang, D. Zhu, P. Li, Z. Su, B. Li, Solid State Electron. 69 (2012) 67–71.
[87] F. Wei, G.-X. Yu, J. Lumin. 134 (2013) 710–717.
[88] M. Guan, L. Gao, S. Wang, C. Huang, K. Wangb, J. Lumin. 127 (2007) 489–493.
[89] Y. Liu, B. Liang, D. Xiao, M. Zhu, W. Zhu, J. Alloys Compd. 469 (2009) 370–373.
[90] Z. Chen, F. Ding, F. Hao, M. Guan, Z. Bian, B. Ding, C. Huang, N. J. Chem. 34 (2010) 487–494.
[91] A.N. Gusev, V.F. Shul'gin, S.B. Meshkova, P.G. Doga, M. Hasegawa, G.G. Aleksandrov, I.L. Eremenko, W. Linert, Inorg. Chim. Acta 387 (2012) 321–326.
[92] A.N. Gusev, M. Hasegawa, G.A. Nishchymenko, V.F. Shul'gin, S.B. Meshkova, P. Doga, W. Linert, Dalton Trans. 42 (2013) 6936–6943.
[93] A.N. Gusev, M. Hasegawa, V.F. Shul'gin, G. Nishchymenko, W. Linert, Inorg. Chim. Acta 414 (2014) 71–77.
[94] A.N. Gusev, V.F. Shul'gin, G. Nishimenko, M. Hasegawa, W. Linert, Synth. Met. 164 (2013) 17–21.
[95] C.R. De Silva, J.R. Maeyer, A. Dawson, Z. Zheng, Polyhedron 26 (2007) 1229–1238.
[96] L. Panayiotidou, M. Stylianou, N. Arabatzis, C. Drouza, P. Lianos, E. Stathatos, A.D. Keramidas, Polyhedron 52 (2013) 856–865.
[97] G.-L. Law, K.-L. Wong, H.-L. Tam, K.-W. Cheah, W.-T. Wong, Inorg. Chem. 48 (2009) 10492–10494.
[98] W. Hu, M. Matsumura, M. Wang, L. Jin, Appl. Phys. Lett. 77 (2000) 4271–4273.
[99] E.E.S. Teotonio, H.F. Brito, M. Cremona, W.G. Quirino, C. Legnani, M.C.F.C. Felinto, Opt. Mater. 32 (2009) 345–349.
[100] H. Xu, L.H. Wang, X.H. Zhu, K. Yin, G.Y. Zhong, X.Y. Hou, W. Huang, J. Phys. Chem. B 110 (2006) 3023–3029.
[101] D.B. Ambili Raj, S. Biju, M.L. Reddy, Dalton Trans. (2009) 7519–7528.
[102] D.B. Raj, B. Francis, M.L. Reddy, R.R. Butorac, V.M. Lynch, A.H. Cowley, Inorg. Chem. 49 (2010) 9055–9063.
[103] M. Pietraszkiewicz, M. Maciejczyk, I.D.W. Samuel, S. Zhang, J. Mater. Chem. C 1 (2013) 8028–8032.
[104] H. Xu, K. Yin, L. Wang, W. Huang, Thin Solid Films 516 (2008) 8487–8492.
[105] H. Xu, Y. Wei, B. Zhao, W. Huang, J. Rare Earths 28 (2010) 666–670.
[106] H. Xu, K. Yin, W. Huang, Chem. Eur. J. 13 (2007) 10281–10293.
[107] K. Yin, H. Xu, G. Zhong, G. Ni, W. Huang, Appl. Phys. A 95 (2009) 595–600.
[108] H. Xu, K. Yin, W. Huang, ChemPhysChem 9 (2008) 1752–1760.
[109] H. Xu, K. Yin, W. Huang, J. Phys. Chem. C 114 (2010) 1674–1683.
[110] J. Wang, C. Han, G. Xie, Y. Wei, Q. Xue, P. Yan, H. Xu, Chem. Eur. J. 20 (2014) 11137–11148.
[111] C. Han, L. Zhu, F. Zhao, Z. Zhang, J. Wang, Z. Deng, H. Xu, J. Li, D. Ma, P. Yan, Chem. Commun. 50 (2014) 2670–2672.
[112] C. Han, F. Zhao, Z. Zhang, L. Zhu, H. Xu, J. Li, D. Ma, P. Yan, Chem. Mater. 25 (2013) 4966–4976.
[113] C. Han, Z. Zhang, H. Xu, G. Xie, J. Li, Y. Zhao, Z. Deng, S. Liu, P. Yan, Chem. Eur. J. 19 (2013) 141–154.
[114] L.-H. Xie, C.-R. Yin, W.-Y. Lai, Q.-L. Fan, W. Huang, Prog. Polym. Sci. 37 (2012) 1192–1264.
[115] J.M. Stanley, B.J. Holliday, Coord. Chem. Rev. 256 (2012) 1520–1530.
[116] H. Yan, H. Wang, P. He, J. Shi, M. Gong, Synth. Met. 161 (2011) 748–752.
[117] S. Fan, X. Fei, X. Wang, J. Tian, L. Xu, P. Yang, Y. Wang, React. Funct. Polym. 76 (2014) 19–25.
[118] C.-J. Xu, B.-G. Li, Macromol. Chem. Phys. 211 (2010) 1733–1740.
[119] H. Yan, H. Wang, P. He, J. Shi, M. Gong, Inorg. Chem. Commun. 14 (2011) 1065–1068.

[120] M. Yang, Q. Ling, M. Hiller, X. Fun, X. Liu, L. Wang, W. Zhang, J. Polym. Sci. A 38 (2000) 3405–3411.
[121] Q.D. Ling, Q.J. Cai, E.T. Kang, K.G. Neoh, F.R. Zhu, W. Huang, J. Mater. Chem. 14 (2004) 2741–2748.
[122] Z.-G. Zhang, J.-B. Yuan, H.-J. Tang, H. Tang, L.-N. Wang, K.-L. Zhang, J. Polym. Sci. A 47 (2009) 210–221.
[123] C. Yang, J. Xu, Y. Zhang, Y. Li, J. Zheng, L. Liang, M. Lu, J. Mater. Chem. C 1 (2013) 4885–4901.
[124] H. Xu, R. Zhu, P. Zhao, L.-H. Xie, W. Huang, Polymer 52 (2011) 804–813.
[125] H. Xu, R. Zhu, P. Zhao, W. Huang, J. Phys. Chem. C 115 (2011) 15627–15638.
[126] J. Pei, X.-L. Liu, W.-L. Yu, Y.-H. Lai, Y.-H. Niu, Y. Cao, Macromolecules 35 (2002) 7274–7280.
[127] X.-Y. Chen, X. Yang, B.J. Holliday, J. Am. Chem. Soc. 130 (2008) 1546–1547.
[128] G.-A. Wen, X.-R. Zhu, L.-H. Wang, J.-C. Feng, R. Zhu, W. Wei, B. Peng, Q.-B. Pei, W. Huang, J. Polym. Sci. A 45 (2007) 388–394.
[129] D.A. Turchetti, P.C. Rodrigues, L.S. Berlim, C. Zanlorenzi, G.C. Faria, T.D.Z. Atvars, W.H. Schreiner, L.C. Akcelrud, Synth. Met. 162 (2012) 35–43.
[130] Y.S.L.V. Narayana, S. Basak, M. Baumgarten, K. Müllen, R. Chandrasekar, Adv. Funct. Mater. 23 (2013) 5875–5880.
[131] S. Basak, Y.S.L.V. Narayana, M. Baumgarten, K. Muellen, R. Chandrasekar, Macromolecules 46 (2013) 362–369.
[132] H. Xu, J. Wang, Y. Wei, G. Xie, Q. Xue, Z. Deng, W. Huang, J. Mater. Chem. C 3 (2015) 1893–1903.